Final report

1. Project details

Project title	PowerKey – Enhanced wind turbine control for optimized wind power plant operation
File no.	12558 (?)
Name of the funding scheme	ForskEL
Project managing company / institution	DTU Wind Energy
CVR number (central business register)	
Project partners	-
Submission date	27 September 2022

2. Summary

Describe the objectives of the project, the obtained results and how they will be utilized in the future.

The short description should be in two versions:

- *English version*
- *Danish version*

Each version should be brief, no more than 2000 characters (including spaces).

The control objective of wind turbine control is to reduce the cost of wind energy. This is typically achieved by maximising power output and reducing fatigue and extreme loads of key turbine components that prolongs the lifetime of turbines. However, in the recent decade, more wind turbines are installed together in wind turbine clusters, and the aerodynamic wake interaction could potentially have an impact on the energy yield and increase the structural degradation on the turbines. Moreover, with an increasing amount of wind energy being connected to the electrical grid, the traditional 'greedy' control strategy of the individual wind turbine might not be the 'optimal' strategy to reduce the cost of wind energy coming from wind farms. The best control strategy might need to take into account the electrical grid information combined with wind farm conditions.

In this project, we developed control solutions that enable turbines to be aware of the grid condition/requirements (e.g. perform down-regulation if necessary) or reserve a certain amount of power in the wind and generate when needed (e.g. by employing wind speed estimator to predict the available power). In addition, some

control solutions enable turbines to operate in such a way that the generated wake effect is minimized for the downstream turbines. (e.g. min Ct strategy). Another control method we studied can enable turbines to reduce tower loading when the turbulence level is high. In addition, model predictive control was investigated, enabling the turbine to be aware of the operating constraints. Those control strategies are not only published in conference proceeding and journals but also implemented in the open-source DTU Wind Energy Controller.

Regarding experimental activities and demonstration, the project obtained wind measurement data from the Vestas V52 test turbine at Risø, where the data is generated with the turbine in a yaw position as well as operated down-regulated. These wind measurements are particularly valuable for studying turbines operating in a wind farm.

Danish version

Formålet med regulering af vindmøller er at reducere omkostningerne ved produktion af vindenergi. Dette opnås typisk ved at maksimere effekten og reducere udmattelses belastning såvel som ekstrem belastning af vigtige møllekomponenter, og dermed forlænge møllernes levetid. Indenfor de seneste årti'er har man iagttaget en udvikling, hvor møllerne i stigende grad placeres i såkaldte vindmølleparker, hvor møllerne placeres relativt tæt sammen. Med begrænset indbyrdes afstand vil de enkelte møller påvirke hinanden aerodynamisk, idet kølvandet fra opstrøms møller potentielt vil have en negativ indflydelse på energiudbyttet fra nedstrøms møller samt øge den strukturelle belastning af disse. I sådanne vindparker er den traditionelle 'grådige' kontrolstrategi for den enkelte mølle forventeligt ikke den 'optimale' strategi for at reducere omkostningerne til vindenergi fra vindparker. Hertil kommer er et yderligere aspekt knyttet til elnettet generelt. Med en stigende mængde af vindenergi forbundet til elnettet, skal den optimale kontrolstrategi af en vindpark også inkludere information om og fra elnettet , og med dette udgangspunkt fastlægge en optimal strategi for vindparkens drift

I dette projekt udviklede vi kontrolløsninger, der gør det muligt for vindmøller at inddrage information om nettets aktuelle tilstand - f.eks. udføre nedregulering, hvis det er nødvendigt - eller reservere en vis mængde energi i vinden og generere strøm af dette, når det er nødvendigt. Dette kan eksempelvis opnås ved at at anvende en vindhastighedsestimator til at forudsige den tilgængelige kinetiske energi i vinden og dermed estimere størrelsen af en endnu ikke udnyttet strømproduktione. Derudover gør nogle kontrolløsninger det muligt for møller at fungere på en sådan måde, at påvirkningen hindrørende fra opstrøms genereret kølvand er mindst muligt på de nedstrøms møller (f.eks. minimum Ct-strategi). En anden kontrolmetode vi studerede, kan gøre det muligt for vindmøller at reducere tårnbelastningen, når turbulensen er høj. Derudover blev model-prædiktiv kontrol også undersøgt, hvilket gjorde det muligt for møllen at inddrage driftsbegrænsningerne i kontrolalgoritmen. Disse kontrolstrategier er både offentliggjort i konferenceproceedings og i tidsskriftsartikler, og herudover implementeret i DTU Wind Energy's open source Controller.

For så vidt angår fuldskala eksperimentet er DTU's Vestas V52 forskningsmølle på Risø benyttet. Såvel nedregulering og aktiv flytning af nedstrøms kølvand er undersøgt. Dette har stor relevans for møller som er placeret i vindmølleparker. Ved hjælp af avancerede LIDAR (Scanning Light Detection And Ranging) baserede skanning-tekniker, er kølvandet efter V52 møllen monitoreret under når denne møller kører med provokerede yaw-fejl såvel som nedreguleret.

3. Project objectives

- *What was the objective of the project?*
- *Which energy technology has been developed and demonstrated?*

The objective of the project is to develop and test new controller functionalities for addressing the mutual interactions of the WTs through wake effects as well as the ability to respond on grid ancillary service both in simulation and in the field. In other words, the project is to provide an extra set of tools and methods to the wind farm (WF) controller to have full control over the individual wind turbines (WTs) for global power optimization and load reduction. More specifically, the PowerKey project aims to provide additional functionality and flexibility on the optimal "transformation" of such power set points into specific control actions of the individual WTs, in order to extend the limits for optimal WF operation.

WP1 concerns controller development. The objective of WP1 is to develop suitable models of the WT and the wake effect. In addition, this WP aimed to develop WT control strategies to facilitate optimal integrated WF/WT control in supporting ancillary service provisions, grid integration as well as power and load optimization.

WP2 deals with full-scale experimental validation. The objective of WP2 is to test the control strategies and tools developed in WP1 on the DTU Vestas V52 research wind turbine located at Risø.

The project developed some key control technologies for wind turbines that takes into account the grid condition and wind farm situations. The developed control technology can ensure that the turbines are operating in a co-operative fashion compared to the typical greedy fashion, where each individual turbine tries to maximise its own energy yield. By operating co-operatively, turbines in a wind farm can collectively generate the maximum power output, and the key turbine components can have a relatively long lifetime.

Moreover, the effect of turbine down-regulation has been demonstrated in the WP2 of the project. The LiDAR systems were employed to measure the wake characteristics behind the turbine rotor when running in a de-rated state In addition, another experiment was to investigate the wake behaviour of yawed turbine. By misaligning the turbine with the dominant wind direction, the downstream wake would be steered away from where it should be otherwise. Thus, if there was a downstream turbine, it will generate more power and experience less fatigue due to the mitigating effect of the wake.

4. Project implementation

- *How did the project evolve?*
- *Describe the risks associated with conducting the project.*
- *Did the project implementation develop as foreseen and according to milestones agreed upon?*
- *Did the project experience problems not expected?*

PowerKey was a three years project. The project was successfully implemented. The project results have been disseminated in reputable international journals and conferences. Moreover, some of the works have already

been utilised in a bigger scale EU project, TotalControl. The experimental validation also went well. The project obtained some good wind and wake measurements of the Vestas V52 at Risø.

Nonetheless, three years is a long time period, and some unforeseeable but low-risk issues would inevitably occur. The first and obvious one was that there has unfortunately been several replacements within the project leader position. Below a short summary of the situation:

- Original project leader: Kenneth Thomsen, left for a position at Envision energy.
- Project leader 2: Mahmood Mirzaei, left for a position at Vestas Wind systems.
- Project leader 3: Rasmus Holm, left for a position at Siemens-Gamesa.
- Project leader 4: Alan Wai Hou Lio (Interim project leader Torben Juul Larsen Aug- Dec 2018 due to medical leave of Alan Wai Hou Lio).

The second issue was that in WP2, the test turbine controller could not be modified as also mentioned in our yearly report. Searching for an alternative turbine is beyond the timeline and budget of this project. The task was then focused on experiments that do not require a major reconfiguration of the controller such as wake measurement with different power set-point and yaw settings and verification of different estimated schemes.

5. Project results

- *Was the original objective of the project obtained? If not, explain which obstacles that caused it and which changes that were made to project plan to mitigate the obstacles.*
- *Describe the obtained technological results. Did the project produce results not expected?*
- *Describe the obtained commercial results. Did the project produce results not expected?*
- *Target group and added value for users: Who should the solutions/technologies be sold to (target group)? Describe for each solutions/technology if several.*
- *Where and how have the project results been disseminated? Specify which conferences, journals, etc. where the project has been disseminated.*

The project objective is to develop and validate new controller functionalities that understand the aerodynamic wake interactions between turbines and moreover has the ability to respond on grid ancillary service demands. The aim was to develop and test these functionalities both in simulation and in the field.

Most of the tasks were successfully completed. See the reports of the deliverables. The project developed a number of key control solutions for turbines that understand the grid condition and the wind farm situation.

Notice that only some of the results are presented in this report.

5.1 Down-regulation strategies

Three derating strategies were proposed where the turbine operates in different rotor speed set-point and generator torque set-point, if down-regulation is required from the grid. The fatigue loads of each strategy was fully investigated.
The power produced by a turbine is the generator torque times the generator speed. Down-regulation can be achieved by either manipulating the generator torque or rotor speed set-point (Mirzaei et al., 2014). Therefore, the first two types of methods are torque-based and rotor-speed-based down-regulation strategies.

Torque-based down-regulation strategy The torque-based strategy performs turbine down-regulation by changing the generator torque input solely. One of the benefits of such a strategy is that during power curtailments, the rotor speed is operating at rated and thus reserving the maximum amount of spinning energy for providing fast frequency response support to the grid (Aho et al., 2012). To implement the torque-based strategy, a new maximum torque limit derated $\bar{\tau}_{\mathrm{g,derated}}$ is imposed on the generator torque in (3c), defined as follows:

$$\bar{\tau}_{\mathrm{g,derated}} = \frac{P_{\mathrm{derated}}}{\omega_{\mathrm{rated}}}$$

where P_{derated} denotes derating power set-point and ω_{rated} denotes the rated rotor speed.

Rotor-speed-based down-regulation strategy In this strategy, down-regulation is performed by defining the rotor speed set-point and the generator torque is updated accordingly. There are numerous advantages to this strategy. For example, the turbines operating in lower rotor speed produce lower noise and also lower fatigue loads on the tower (W. H. Lio et al., 2018). To perform the rotor-speed-based strategy, the original rated rotor speed and generator torque limit needs to be modified as follows:

$$\omega_{\mathrm{derated}} = \sqrt[3]{\frac{P_{\mathrm{derated}}}{K_{\mathrm{opt}}}},\ \bar{\tau}_{\mathrm{g,derated}} = \frac{P_{\mathrm{derated}}}{\omega_{\mathrm{derated}}}$$

where $\omega_{\mathrm{derated}}$ denotes the derating rotor speed set-point to the controller.

Figure 1 depicts the operating trajectories of the normal and down-regulation strategies under various wind conditions. At low wind speeds, three trajectories are identical with high tip-speed ratios and optimal pitch angles. In contrast, at high wind speeds, the trajectories are different based on the control strategies. Figure 2 shows typical steady-state values of the DTU 10 MW reference wind turbine (RWT) (Bak et al., 2013) for the power, rotor speed, pitch and generator torque in both normal and down-regulation situations. Notice that the gearbox ratio is 1. Two down-regulation strategies are the torque-based and rotor-speed-based strategies and their derating operating points compared to the normal operations are shown in Fig. 3.

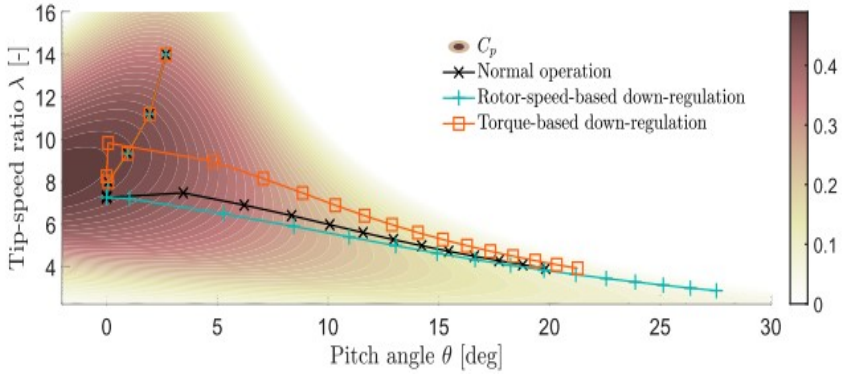

Figure 1 - Operational steady-states of various control strategies on the Cp surface.

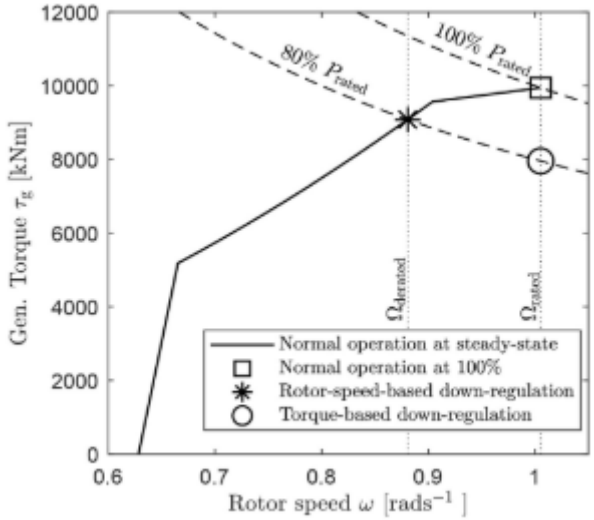

Figure 2 - Torque versus rotor speed curve of the DTU 10 MW RWT in normal operation and down-regulation. In torque-based down-regulation, the turbine operates at 80% of the rated power and rated rotor speed. In rotor-speed-based down- regulation, the turbine rotor speed is regulated around a derated rotor speed.

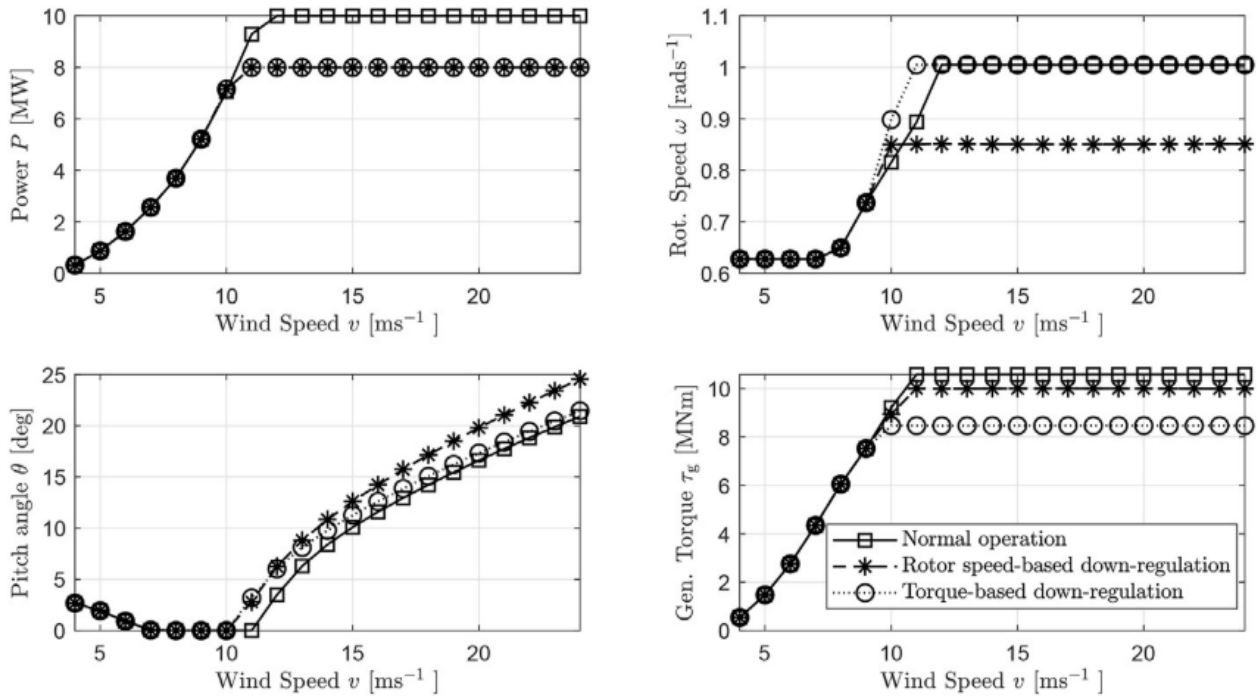

Figure 3 - Typical steady-state conditions of the DTU 10 MW RWT in normal operation and down-regulations. In two down-regulation cases, the turbines are operating at 80% of the rated power. The rated generator power is 10 MW as shown in top-left figure.

Minimum Ct derating strategy

Details can be found in (Meng et al., 2020)

Besides the two down-regulation strategies (torque-based and rotor-speed-based), there is another type of derating strategy called the minimum Ct control strategy, which minimizes the thrust coefficient of a turbine for a given power output. This control strategy, although reducing the power output of the de-rated turbines, results in an overall increase in power output in the wind farm due to attenuated wake effects. An additional benefit of minimum Ct control is a reduction of fatigue loads farm-wide due to a reduction of the wake deficit and added wake turbulence mentioned in (Ma et al., 2017; Zhu et al., 2017)

The concept of minimum Ct control strategy is described in the optimisation problem (1).
For a given down regulation percentage, ΔP, the following minimization problem is solved to find the solution of tip-speed-ratio, λ, and pitch angle, β. The power coefficient, Cp, and thrust coefficient, Ct, of the DTU 10MW reference turbine are illustrated in contour plots as functions of λ and β in Figure 4.

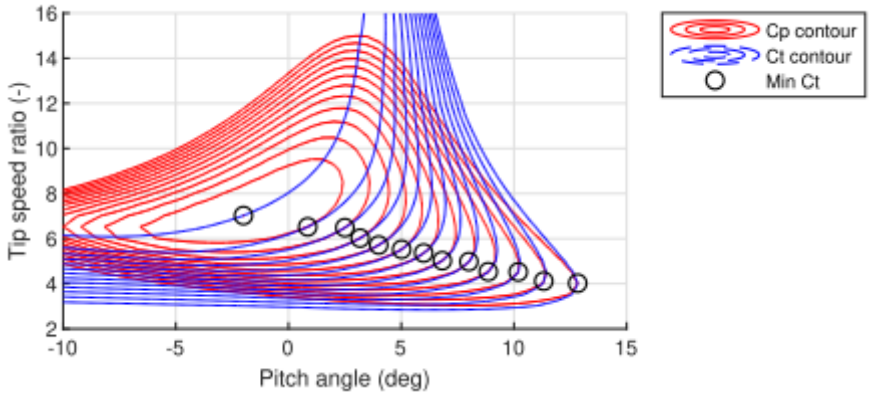

Figure 4 - Cp, Ct contours and minimum Ct operational points.

The calculated values of λd and βd that satisfy minimum Ct requirement are plotted in Figure 4 and marked as black circles. The power coefficient, Cp,d, associated with down regulation percentage is tabulated as a function of λd and βd and will be used when calculating the generator constant K in Equation 2.

$$\lambda_d, \beta_d = \arg\min_{\lambda,\beta} C_t(\lambda, \beta)$$

$$\text{Subject to: } \begin{cases} C_{p,d}(\lambda_d, \beta_d) = \Delta P C_{p,max} \\ \lambda_{min} \leq \lambda_d \leq \lambda_{max} \\ \beta_{min} \leq \beta_d \leq \beta_{max} \end{cases} \quad (1)$$

We utilize the same terminology as defined in literature , where the control regions are referred to as Rgions 2, 2.5 and 3. The implementation of this control strategy in Region 2 is simply re-calculating the generator constant, K, tracking the minimum Ct instead of the traditional way that tracks the optimal power coefficient Cp,max using the equation

$$K = \frac{1}{2}\rho\pi R^5 \left(\frac{1}{N\lambda_d}\right)^3 C_{p,d}(\lambda_d, \beta_d) \quad (2)$$

where, N is the gearbox ratio, R is the rotor radius, ρ is air density and Cp,d is the power coefficient value associated with down regulation percentage. In Region 2.5, a PI generator torque controller with torque limits is implemented. We assume the rated wind speed (Vr) is the same as the designed value. Then, the lower limit of generator speed in Region 2.5, Ω2.5, is calculated as

$$\Omega_{2.5} = \frac{V_r \lambda_d}{R} \quad (3)$$

where, λd is the tip-speed-ratio value as the solution of the minimization problem mentioned before. The upper limit generator speed in Region 2.5 during down regulation, which is the de-rated generator speed in Region 3, is defined as Ωr,d = Ω2.5/γ. Here, the γ is an user selected parameter. In this study, a value of 95% is used for generalizing the minimum Ct control strategy to match the behavior

of the DTU Basic Controller when the down-regulation level is at 100%. A linear interpolation factor, σ, is defined as

$$\sigma\left(\Omega_{2.5}, \Omega_{r,d}; \Omega\right) = \begin{cases} 0 & \Omega < \Omega_{2.5}, \\ \frac{\Omega - \Omega_{2.5}}{\Omega_{r,d} - \Omega_{2.5}} & \Omega_{2.5} \leq \Omega \leq \Omega_{r,d}, \\ 1 & \Omega > \Omega_{r,d}, \end{cases} \tag{4}$$

where, Ω is the current generator speed. Then, the torque limits used by the PI generator torque controller in Region 2.5 is expressed as

$$Q_g \in \begin{cases} [K\Omega^2, K\Omega^2] & \Omega < \Omega_{2.5}, \\ [K\Omega_{2.5}^2, (1-\sigma)K\Omega^2 + \sigma Q_{g,r}^d] & \Omega_{2.5} \leq \Omega \leq \Omega_{r,d}, \\ [Q_{g,r}^d, Q_{g,r}^d] & \Omega > \Omega_{r,d}, \end{cases} \tag{5}$$

where, Qd g,r is the de-rated generator torque. In Region 3, The generator speed and torque set-points are determined by Ωr,d and the de-rated generator power. The implementation of the switch between Region 2.5 and 3 follows the same method as described in the report of DTU Wind Energy controller (Hansen & Henriksen, 2013)

Simulation results

Figure 5 shows the 20 years lifetime fatigue loads of the WT-1 operating at wind class IC. As it is shown, most of the fatigue loads are reduced for different down regulation levels compared with normal operation case except for tower bottom fore-aft and side-to-side loads described by channel name TBFA and TBSS, and the yaw bearing roll moment and main bearing torsional moment described by channel name YBRoll and MBTor, which are related to the drive train loads. The blade root edgewise bending moment is mainly driven by the gravity, therefore, the edgewise fatigue load reduction is smaller compared to the flapwise fatigue load.

A further investigation on the time series and the Fast Fourier Transformed (FFT) signal of tower bottom fore-aft bending moment (see Figure 3) shows that the fatigue load increase at the tower bottom for fore-aft bending moments is due to higher oscillation when the turbine is de-rated. This is caused by the 3P frequency (0.255 Hz) interaction with the tower fore-aft (0.25 Hz) frequency of this DTU 10MW turbine when the turbine is de-rated to 70% with the rotor speed at 5.1 rpm. Figure 6 shows, at 10 m/s, when the turbine is running without de-rating, the 3P frequency is 0.4 Hz. The 3P frequency is reduced to 0.281 Hz and 0.255 Hz when the turbine is de-rated at 90% and 70% respectively. Therefore, when the turbine is de-rated, for example, at 90% and 70%, the tower fore-aft mode is excited and a higher amplitude as it is shown in Figure 6 is observed. Similar resonance phenomena is observed for the tower side-to-side mode in Figure 7. Further more, the excited tower side-to-side vibration couples with the drive train torsional mode and leads to higher drive train torsional oscillation, which is closely related to the main bearing torsional moment (MBTor) and the yaw bearing roll moment (YBRoll). This explains the fatigue loads increase on channels YBRoll and MBTor.

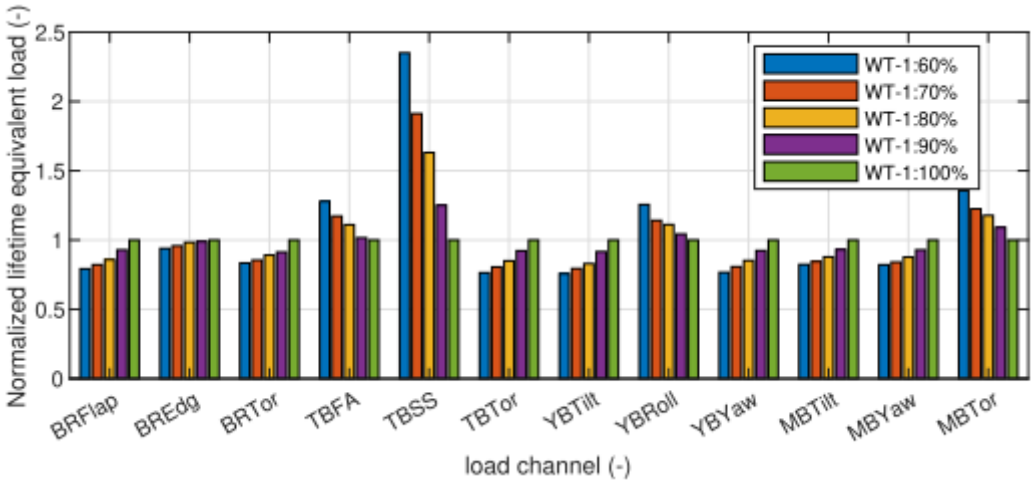

Figure 5 - 20 years normalized damage equivalent loads on WT-1 for wind class IC.

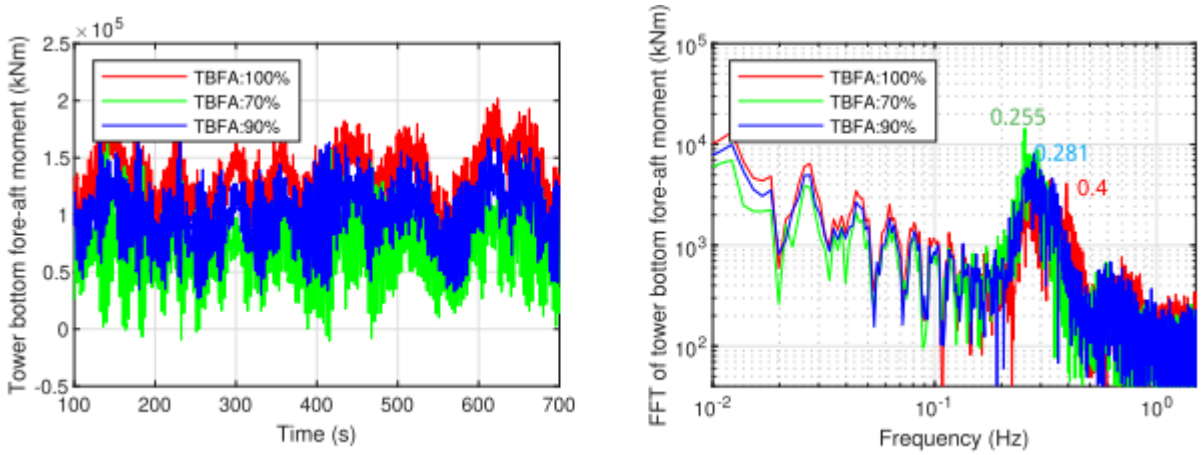

Figure 6 - Time series and FFT of the tower bottom fore-aft bending moment at 10 m/s.

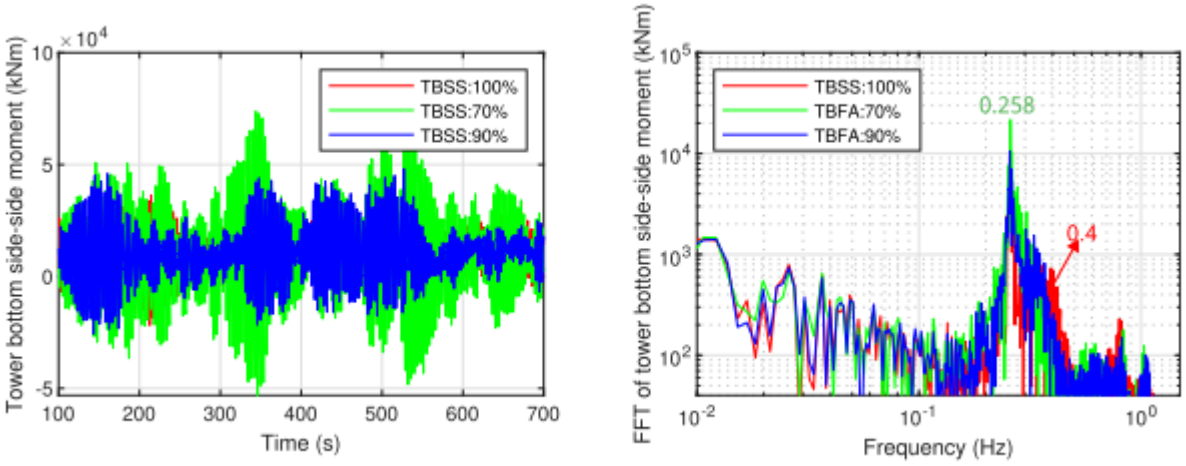

Figure 7 - Time series and FFT of the tower bottom side-side bending moment at 10 m/s.

This finding suggests that for the turbines designed with narrow rotor speed range, like the DTU 10MW reference turbine, with the range from 6 rpm to 9.6 rpm, the rotor speed exclusion should be implemented in the down regulation control algorithm to avoid resonance. It also suggests that the drive train damping parameters need to be re-tuned in order to damp the drive train vibration under the down-regulated control. Re-tuning of the drive train damping parameters for down regulation is out of the range of this investigation

5.2 Gain-scheduling controller in down-regulation

A novel gain-scheduling method was proposed to improve the loading of the turbine, as described in the report (Deliverable 2). Also, more details can be found in (W. H. Lio et al., 2019)

Considering the simplified non-linear drive-train dynamics of the turbine, assuming the shaft is rigid, defined as follows:

$$J_{\mathrm{r}}\dot{\Omega}(t) = \tau_{\mathrm{a}}(\Theta, V, \Omega) - \tau_{\mathrm{g}}(\Omega),$$

where Ω(t), Jr denote the rotational speed and inertia of the blade-pitch angle Θ(t), wind speed V(t) and rotor torque τa(Θ, V, Ω) : R×R×R → R is a non-linear function the above-rated wind conditions is defined as follows: speed Ω(t), whilst the generator torque τg(Ω) : R →R is defined as follows:

$$\tau_{\mathrm{g}}(\Omega) = \frac{P_{\mathrm{sp}}}{n_{\mathrm{gb}}\Omega},$$

where Psp is the set-point of the power. By linearisation, the aerodynamic torque becomes:

$$\tau_{\mathrm{a}}(\Theta, V, \Omega)$$
$$\approx \tau_{\mathrm{a}}(\Theta^*, V^*, \Omega^*) + \frac{\partial \tau_{\mathrm{a}}}{\partial \theta}\theta(t) + \frac{\partial \tau_{\mathrm{a}}}{\partial v}v(t) + \frac{\partial \tau_{\mathrm{a}}}{\partial \omega}\omega(t)$$

The linear drive-train model then becomes:

$$J_{\mathrm{r}}\dot{\omega}(t) = \frac{\partial \tau_{\mathrm{a}}}{\partial \theta}\theta(t) + \frac{\partial \tau_{\mathrm{a}}}{\partial v}v(t) + \frac{\partial \tau_{\mathrm{a}}}{\partial \omega}\omega(t) - \frac{\partial \tau_{\mathrm{g}}}{\partial \omega}\omega(t)$$

The typical blade-pitch PI control structure is as follows:

$$\theta(t) = K_{\mathrm{p}}\omega(t) + K_{\mathrm{i}}\int_0^t \omega(\tau)d\tau = K_{\mathrm{p}}\dot{\phi}(t) + K_{\mathrm{i}}\phi(t),$$

where Kp,Ki denote the proportional and integral adopts the pole-placement method for choosing the Kp and Ki (Tibaldi et al., 2015). The pole-placement method is to assign the location of the eigenvalues of the closed-loop systems to achieve certain bandwidth and response. The closed-loop system is defined as follows:

$$J_{\mathrm{r}}\ddot{\phi}(t)+(\frac{\partial\tau_{\mathrm{g}}}{\partial\omega}-\frac{\partial\tau_{\mathrm{a}}}{\partial\omega}-K_{\mathrm{p}}\frac{\partial\tau_{\mathrm{a}}}{\partial\theta})\dot{\phi}(t)-K_{\mathrm{i}}\frac{\partial\tau_{\mathrm{a}}}{\partial\theta}\phi(t)=\frac{\partial\tau_{\mathrm{a}}}{\partial v}v(t).$$

The Kp and Ki give the desired eigenvalues of the closed-loop system (6) are derived as follows:

$$K_{\mathrm{p}}=\frac{2\zeta_{\Omega}\omega_{\Omega}J_{\mathrm{r}}+\frac{\partial\tau_{\mathrm{a}}}{\partial\omega}-\frac{\partial\tau_{\mathrm{g}}}{\partial\omega}}{-\frac{\partial\tau_{\mathrm{a}}}{\partial\theta}},\quad K_{\mathrm{i}}=\frac{\omega_{\Omega}^{2}J_{\mathrm{r}}}{-\frac{\partial\tau_{\mathrm{a}}}{\partial\theta}}$$

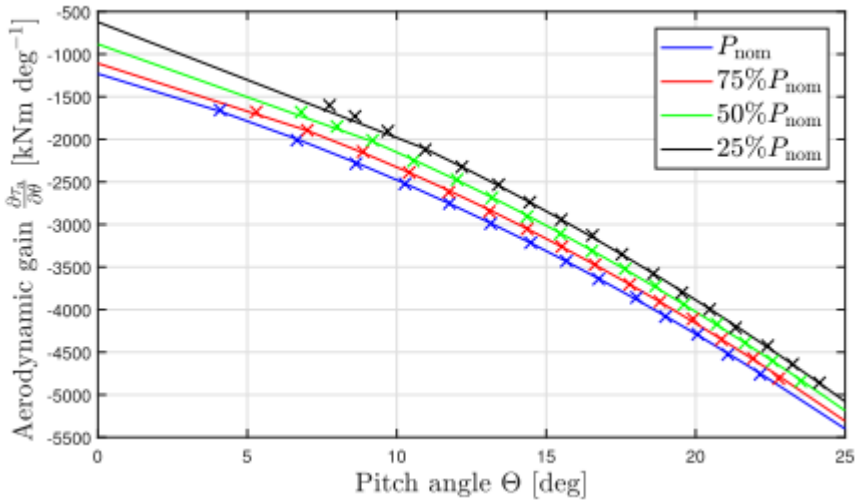

Figure 8 - Aerodynamic gains of the turbine in down- regulation. The crosses and lines show the simulation data and their quadratic approximation.

The aerodynamic gain in down-regulation is shown in Figure 8.The baseline controller will use the aerodynamic gain at Pnom whereas the proposed controller use the aerodynamic gain corresponding to the power set-point.

Simulation results

The turbine model used in this study is the DTU 10MW reference wind turbine upon the HAWC2 platform. This model includes many degrees-of-freedom such as the tower fore-after, side-to-side, in addition to the rotor and blade dynamics. The controller employed in this study is the open-source DTU basic controller with down-regulation feature.

Step-wind

In these closed-loop simulations, two blade-pitch controllers in down-regulation were examined. The power set- point was 75% of the nominal power. The baseline is the controller based on the nominal aerodynamic gains and it is compared with the proposed controller with updates on the aerodynamic gains based on the power demand. Figure 9 shows the sample time history of the rotor speed response, pitch angle and pitch rate subject to a step wind from 11m/s to 12m/s. It is clearly shown

that the pitch activities were better for the proposed controller, with a mere increase in the rotor speed variations.

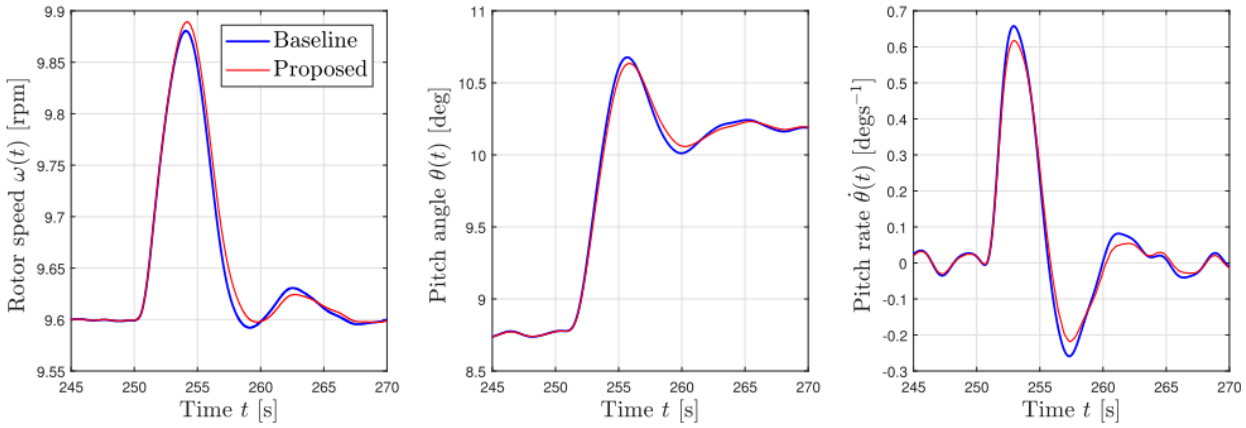

Figure 9 - The sample time histories of the baseline (blue) and proposed (red) controller in down-regulation.

Turbulent wind

The closed-loop simulations were conducted under a turbulent wind field with the mean speed of 16 m/s based on the IEC standard (IEC, 2005). The histograms of the rotor speed and pitch rate variations are shown in Figure 10. The proposed controller achieved reductions in pitch activities and slight increases in the rotor speed variations. Reductions on pitch activities resulted in better attenuation on the tower-base side-side loads, blade flap-wise, edge-wise loads and pitch bearing, with merely increases in the main shaft torsion and tower fore-aft loads.

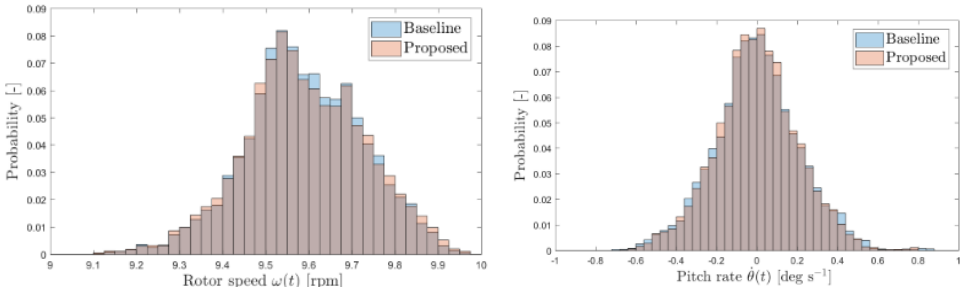

Figure 10 - The histograms of the baseline (blue) and proposed (red) controller in down-regulation.

All these strategies were implemented in the open-source DTU Wind Energy Controller.

https://gitlab.windenergy.dtu.dk/OpenLAC/BasicDTUController

5.3 Rotor effective wind speed estimator

A wind speed estimator was developed in this project. The estimator can infer the wind speed from standard measurements of a wind turbine such as rotor speed, pitch angle and generator torque.

Based on the estimated wind speed, the power available in the wind can be estimated, which is particularly important for power reserve control. The power reserve is an important feature for wind energy, as wind energy becomes larger in the energy mix. By reserving some generation capacity, the wind turbine can back the normal operation, if the grid has a sudden need for energy. Thus, the ability to predict wind speed is crucial for this application. The wind speed estimation is also implemented in the open-source DTU Wind Energy Controller.

Methodology can be found in (A. W. H. Lio & Meng, 2020)

Wind speed estimation in down-regulation

Simulation results are presented in this section to investigate the estimation performance for different operating strategies. The reference turbine model is the DTU10MW and the aeroelastic simulation code is HAWC2. The extended Kalman filter based on the turbine model was implemented together with the open-source DTU Basic Controller. The focus of this study is on calculating the power reserve based on the wind estimate, that is particularly important in the below-rated wind region. Thus, two turbulent wind cases with mean wind speeds of 8 m/s (in the middle of the below-rated region) and 11 m/s (around the rated wind speed transition) were considered. Both turbulent intensities were based on IEC standard Class B.

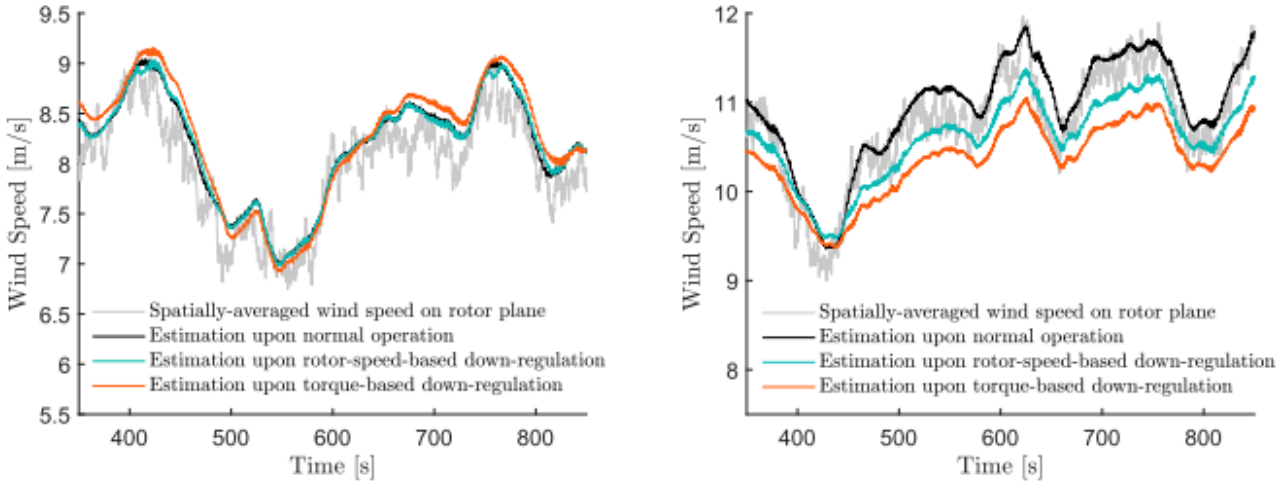

Figure 11 - Time series of the baseline effective wind speed and its estimations under different operating strategies. The left and right plots indicate the results in turbulent wind cases with a mean wind speed of v = 8 m/s and v = 11 m/s, respectively.

Figure 11 shows the effective wind speed estimations under both turbulent wind cases. The baseline is the spatially-averaged wind speed, collected from 9 points across the rotor-plane. Three estimates were shown. The first one was the wind speed estimation in normal operation, whilst the other two were the estimations in down-regulation. The down-regulating turbines were operating at 50% of the rated power. In v = 8 m/s, the estimate from torque-based down-regulating turbines was less accurate than the estimates of the other two strategies, which confirms the observability study. In addition, comparing two figures, the discrepancy between the estimates of all strategies became larger in the high wind speed case. That indicates it is relatively harder to achieve good estimation near or above rated wind region.

Figure 6 shows the time series of the power estimates. For turbines in normal operations, there were good matches between the true power reserve and its estimate in both turbulent wind field. In contrast, the power estimate in the torque-based down-regulation was the worst among other strategies. The mismatch became severer in higher wind speed.

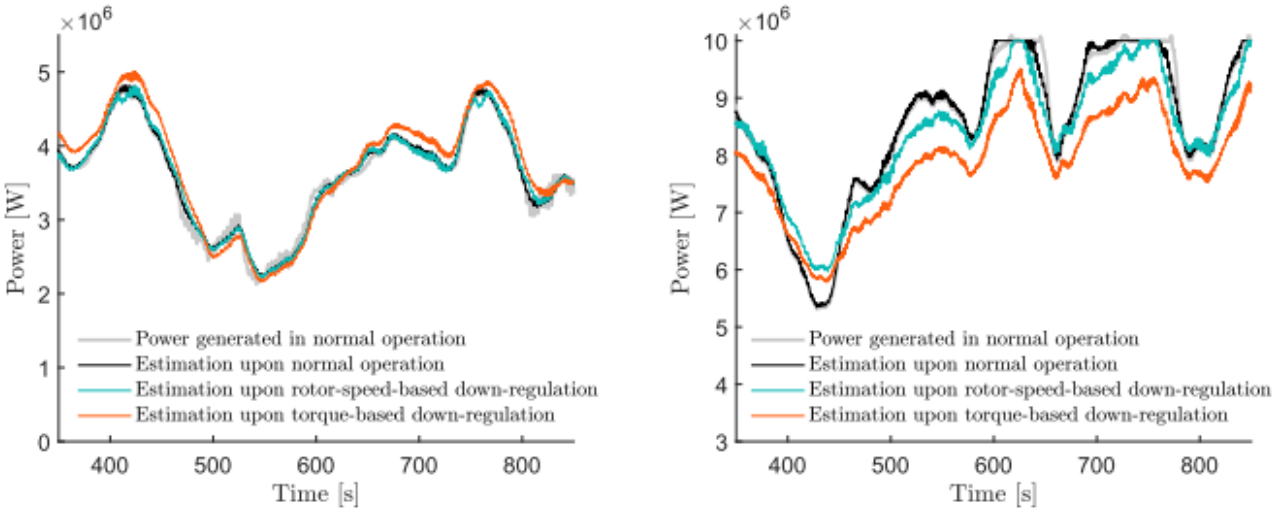

Figure 12 - Time series of the normal power and estimated available power under different control strategies. The left and right plots indicate the results in turbulent wind cases with a mean wind speed of 8 m/s and 11 m/s, respectively

Figure 13 illustrates the histograms of estimation errors in wind speed and power in both wind cases. As expected, the estimation errors in the torque-based down-regulation have a greater degree of dispersion for both wind speed and power estimates. In addition, large peaks at the 0% power estimation error were contributed by the estimate power greater than the rated power. Amongst all strategies, it is clear that the power estimation error for torque- based down-regulation case could be up to ±10%. One interesting observation is that the wind estimate in normal operation was slightly biased.

However, such bias did not reflect in the error of the power estimate under normal operation. This leaves a question whether the spatially-averaged wind speed is a good baseline. The better candidate might be the spatially-weighted wind speed or the wind speed obtained by inverting the power law.

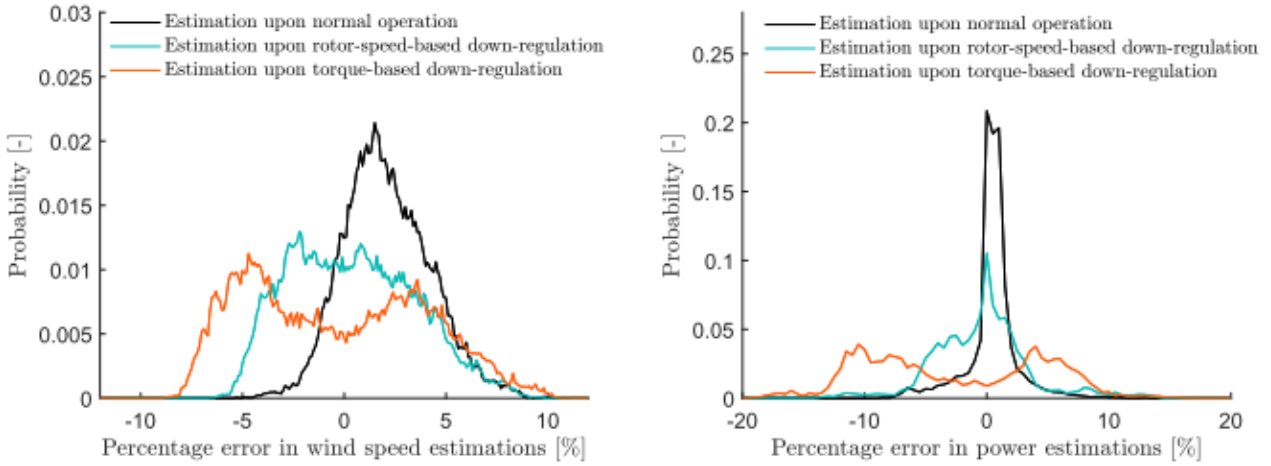

Figure 13 - Histograms of the errors in both turbulent wind cases under different control strategies. The left and right plots show the estimation errors in the wind speed and power, respectively.

5.4 Turbulence-based control

In turbulence-based control, the turbine is able to de-rate for reducing the loading on the tower. The method was evaluated in many different wind cases. The aim of this work is to explore the ways to retain the robustness and performance of controller under different wind conditions for wind turbines. The method of optimizing the control parameters in response to different turbulence intensity is proposed, which is referred to as Adaptive Turbulence-based Control (ATBC). Specifically, the power spectrum of the rotor effective windspeed has been derived and the analytical expression is explicitly considered in control optimization. Also, a linear aero-servo-elastic (ASE) model is established, which captures the closed-loop dynamics of the rotor speed, pitch activity and tower fore-aft vibration mode. Subsequently, a computationally-efficient component damage prediction method is proposed that uses rainflow counting and inverse fast Fourier transform. Based on the proposed AS-model and damage prediction method, the controller optimization problem is established using a quadratic cost function to achieve the optimal trade-off between the rotor speed variation and damage of turbine components. By model validation, it shows the proposed scheme is applicable to predict the component fatigue load and the rotor speed variation in an efficient way. Finally, one design case is given to illustrate the procedure of ATBC and demonstrate the feasibility of the proposed method in different operating wind conditions.

More details can be found in Deliverable Report D3.

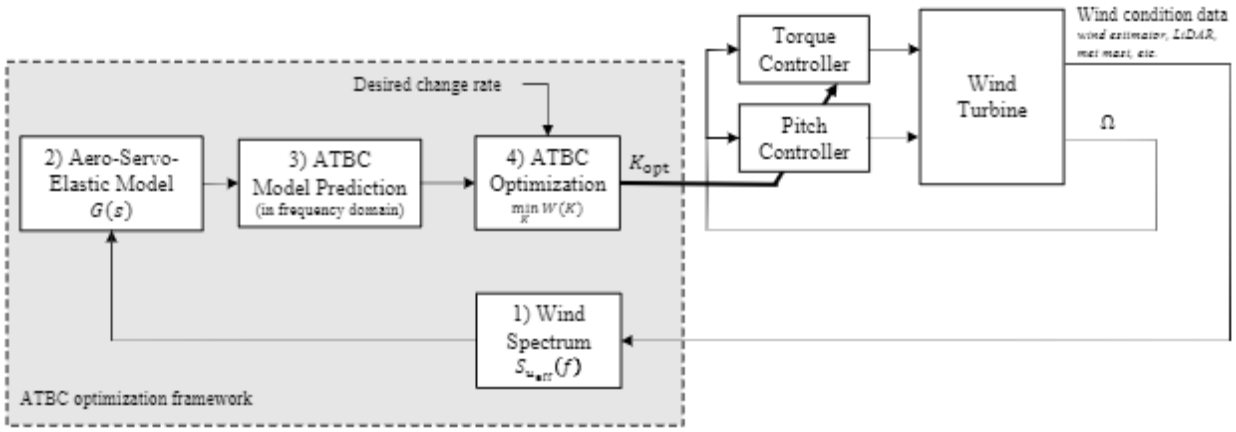

Figure 14 - The framework of adaptive turbulence-based control. Four main parts areincluded: 1) Wind spectrum used to describe the environmental wind condition; 2) Lin-earised wind turbine aero-servo-elastic model; 3) ATBC model in frequency domain provides a quick assessment of the turbine component damage; 4) ATBC optimization function.

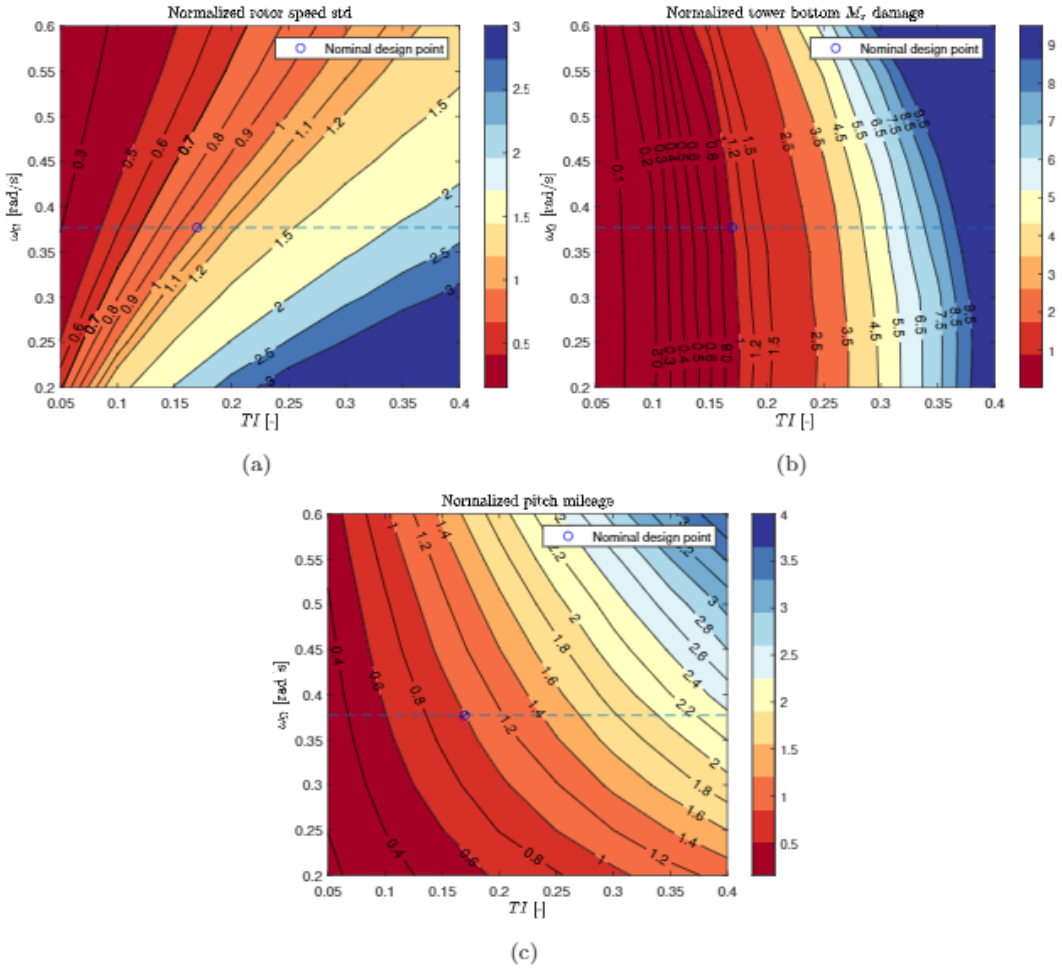

Figure 15 - Adaptive turbulence based control model, $\bar{U}$= 18 m/s. (a) Normalized rotorspeed standard deviation (std); (b) Normalized tower bottom fore-aft bending moment;(c) Normalized pitch mileage.

The prediction performance of the proposed ATBC model is evaluated under a wide range of TI and controller parameters, namely the speed regulator mode frequency. The influence of speed regulator mode

and turbulence intensity on rotor speed variation, tower bottom fore-aft bending moment and pitch mileage are presented in Fig. 15. These are the prediction results based on the RIFFT method that uses the ASE model. The mean wind speed, U is 18 m/s, and the results are normalized over the nominal design point, which is TI = 0.168 andωΩ= 0.377 rad/s for DTU 10 MW RWT. These results provide important insights into the influence of different control setting and TI on specific metrics. The clear trend is highlighted that from higher turbulence intensity follow higher rotor speed variation and higher tower damage. With the increasing ωΩ, the rotor speed variation decreases and tower damage increases. The pitch mileage is quite correlated to the speed regular mode: higher ωΩcauses more pitch actions and higher pitch mileage. The next section, therefore, moves on to validate the proposed model in full nonlinear simulation.

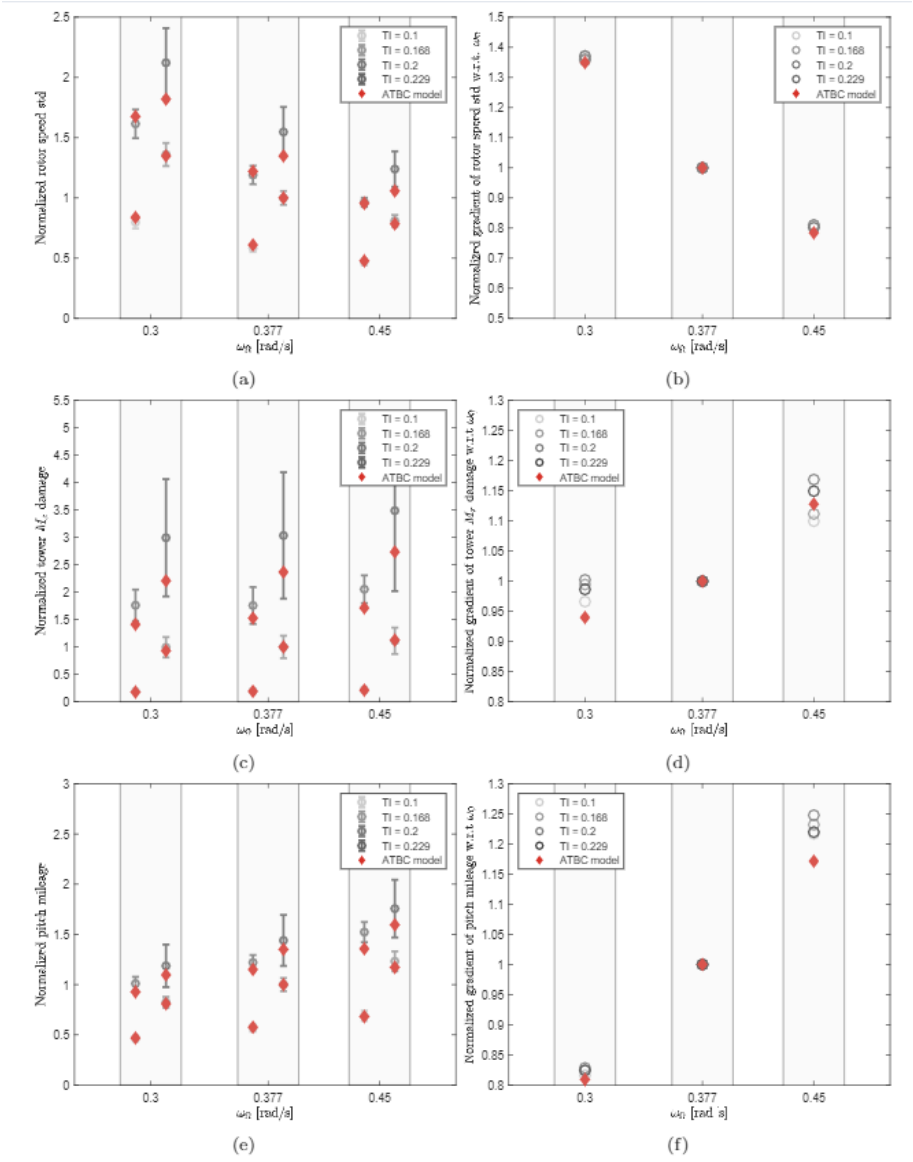

Figure 16 - Comparison between HAWC2 simulation and ATBC model prediction. The mean value and standard deviation of six random seeds in different TI are presented as the round circle and error bar. The color from light gray to dark gray indicates the TI is from low to high. The red diamond is the results from the proposed ATBC model. (a) Normalized rotor speed standard deviation; (b) Normalized gradient of rotor speed std w.r.t. ω_Ω; (c) Normalized tower M_x damage; (d) Normalized gradient of tower M_x damage w.r.t. ω_Ω;(e) Normalized pitch mileage; (f) Normalized gradient of pitch mileage w.r.t. ω_Ω.

Case study

Another potential application of the ATBC model is for the turbine is constantly operating under the extreme turbulence, the rotor speed variation will be high and sometimes will trigger the safety system to shut down the turbine due to overspeed. The ATBC model provides a fast and reliable load assessment which can be used for re-tuning the controller parameter ωΩ, from 0.377 rad/s to 0.45 rad/s, the maximum rotor speed decreases by 4.7% and the peak is below 1.1 rated rotor speed Ωr as presented in Fig. 17.

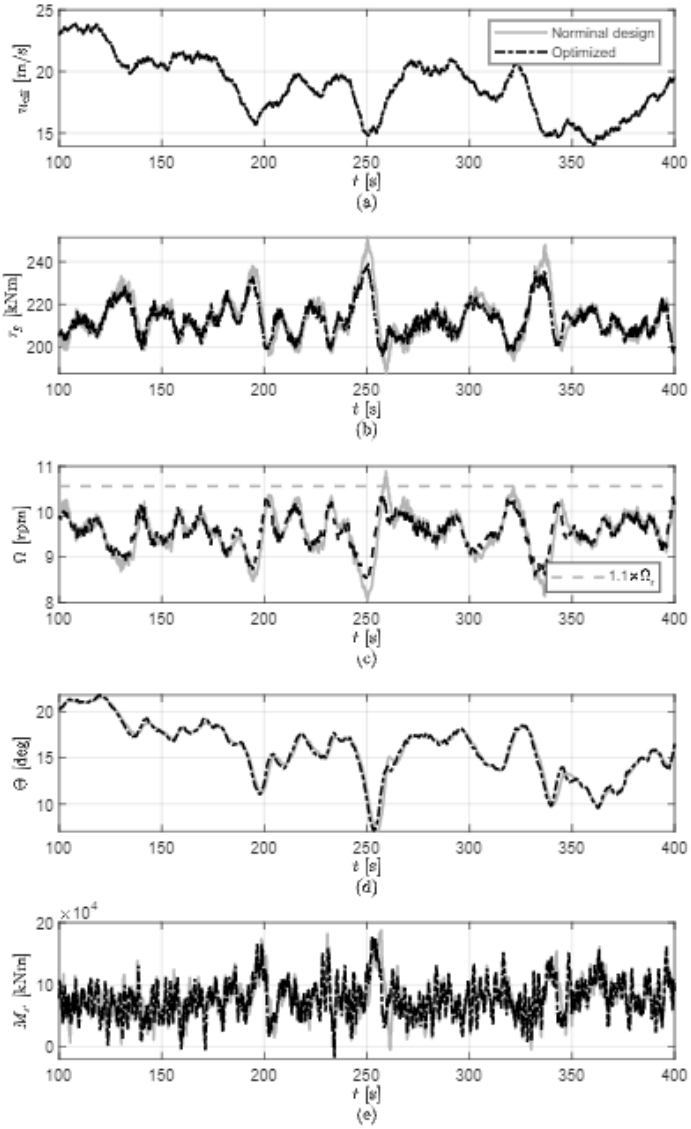

Figure 17 - Comparison of different speed regulator frequency, from nominal designωΩ=0.377 rad/s to optimizedωΩ= 0.45 rad/s,ζΩis kept as 0.7. (a) Rotor averaged windspeed; (b) Generator torque; (c) Rotor speed; (d) Pitch angle; (e) Tower bottom fore-aft bending moment.

5.5 Frequency support capability

A virtual synchronous machine (VSM) control scheme was proposed, which contains a simplified emulation of a conventional power plant for satisfactory frequency support capability. The swing equation and frequency-active power (f-P) droop control are implemented, and in the swing equation the inertia constant is included to regulate the virtual inertial response at the beginning of a frequency event. The proposed VSM control scheme is added to the grid-side converter (GSC) control, together with cascaded inner loops.

Frequency support capability is becoming an important requirement for wind turbines, as wind power is increasingly integrated into power systems. In this paper, a frequency controller is implemented and validated. Such a controller allows wind turbines to help regulate the system frequency automatically and includes virtual inertia to help limit the rate of change of frequency. Compared with other methods, the controller achieves satisfactory frequency support capability with considerable simplicity. The controller is added to the grid-side converter controls, together with cascaded inner loops, which enables wind turbines to operate in grid-forming mode with overcurrent protection. The influence of the controller parameters on the frequency response is investigated.

More details can be found in (Lu et al., 2021). The grid-side converter control scheme is shown in Figure 18.

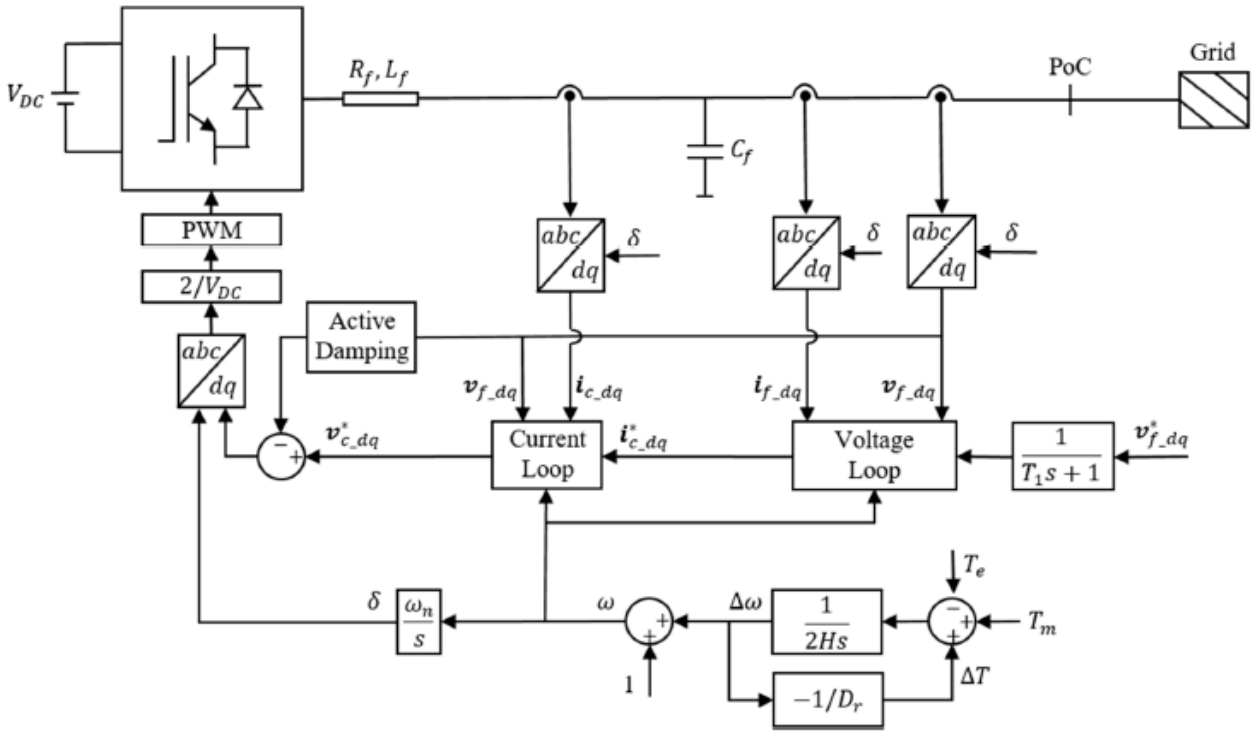

Figure 18 - Investigated grid-side converter (GSC) control scheme.

Simulation results: Influence on Dynamic Response

The influence of the FC's inertia constant and droop coefficient on the system's dynamic response was investigated by performing a parametric sensitivity analysis. The dynamic response of the relevant variables was plotted for different parameter values to assess its influence. Firstly, we varied the value of inertia constant H in the FC, from 2 to 6 W_s/VA, in unitary steps while the droop coefficient Dr was kept constant at 0.05. The results are shown in Figures 19 and 20. Secondly, we changed the value of droop coefficient Dr in the FC from 0.03 to 0.07, with a step of 0.01 while the

inertia constant H was kept constant at 4W_s/VA. The results are shown in Figures 21 and 22. In both cases, the parameters of the SG were not changed. In the figures, the mechanical power of GSC was the active power reference for its controls (Tm + DT in Figure 18).

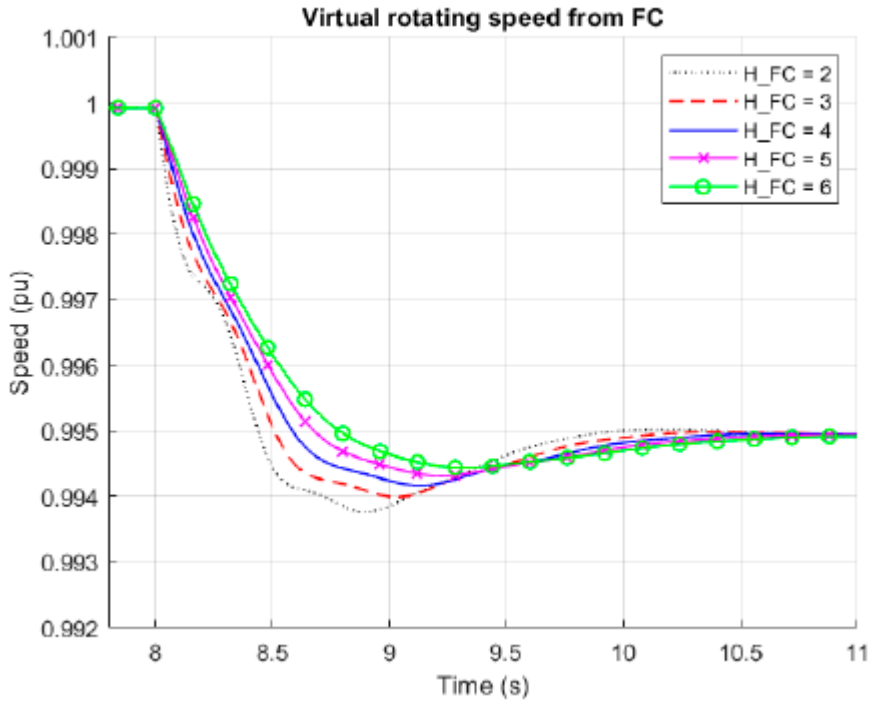

Figure 19 - Influence of the inertia constant H on the virtual rotating speed of FC (H_SG = 4W s/VA)

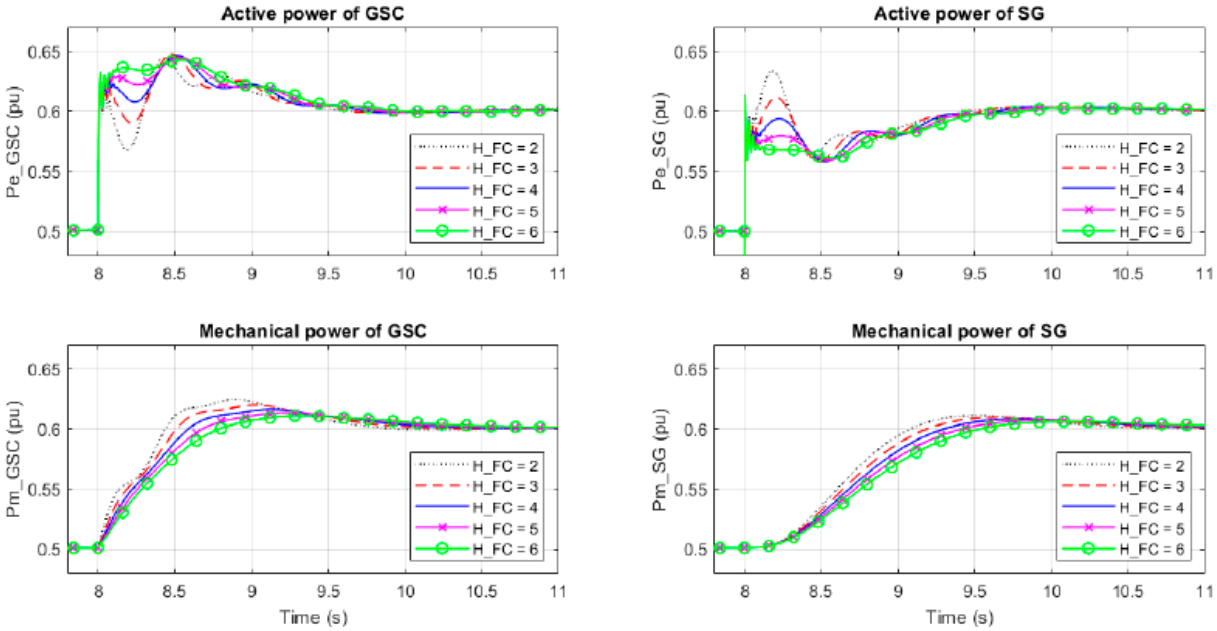

Figure 20 - Influence of the inertia constant H on the system's response (H_SG = 4 W·s/VA, D_FC = D_SG = 0.05).

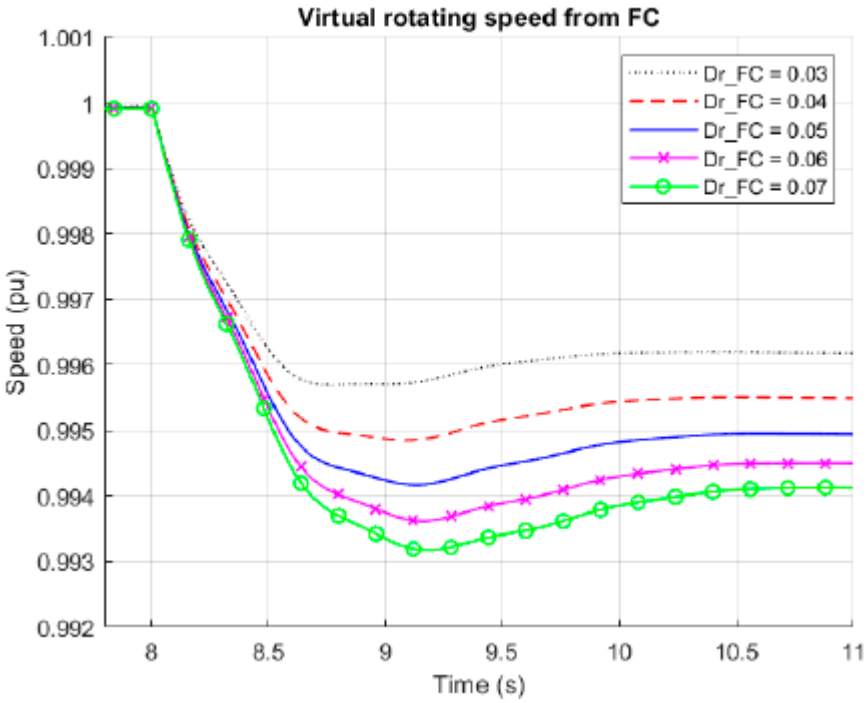

Figure 21 - Influence of the droop coefficient r D on the virtual rotating speed of FC (H_FC = H_SG 4 W s/VA)

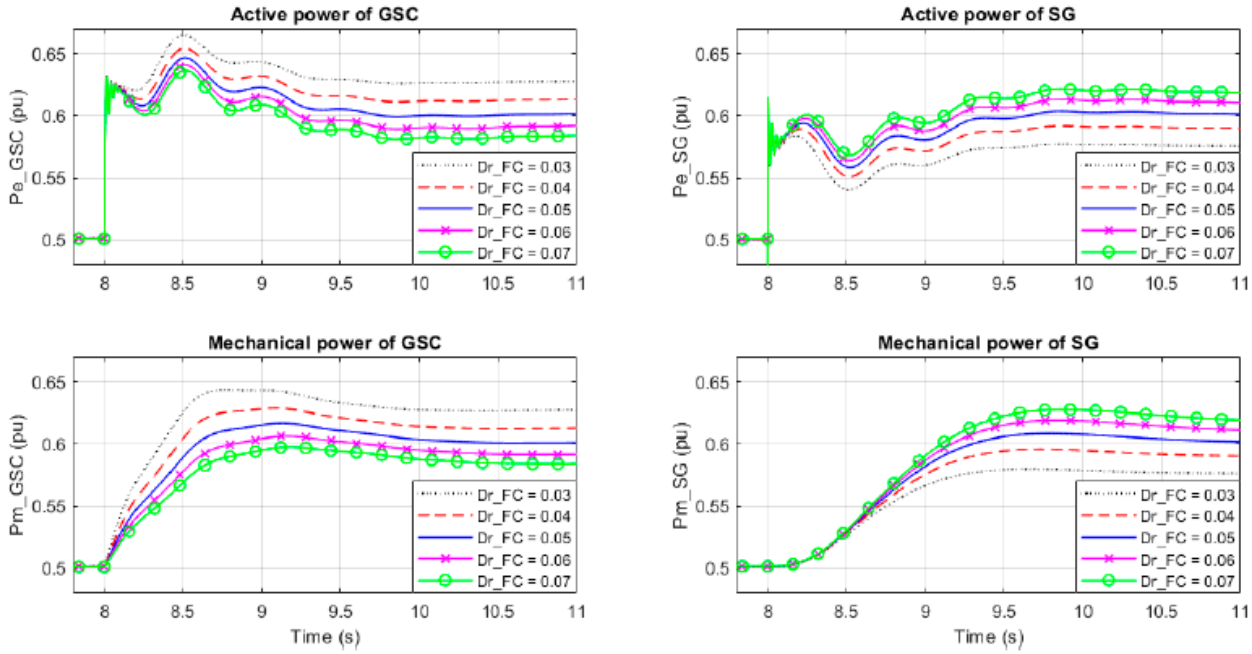

Figure 22 - Influence of the droop coefficient r D on the virtual rotating speed of FC (H_FC = H_SG = 4 W·s/VA)

5.6 Model predictive control

Model predictive control was proposed, where the controller understands the constraint and the incoming wind information. In this project, the model predictive controller imposed a limit on the turbine

tower displacement. Based on these limits, the controller operates the turbine in such a way that the tower load of the turbine was reduced significantly.

This work presents a modular MPC design that works for the full wind speed range based on an existing controller design. The key and distinct features of the MPC such as constraint and preview information handling are incorporated into the existing controller. The proposed MPC design is formulated based on solving an offline inverse optimal control problem. The novelty of the proposed modular MPC is that the design uses the rotor speed measurement as scheduling variable similar to traditional wind turbine controller. Furthermore, the proposed design requires no state observer. Furthermore, tuning of the MPC is straightforward, where the engineers can easily obtain traditional control parameters (e.g. Kp and Ki of the PIDs) that is proven working over time. Most importantly, the proposed method can reduce tower fatigue loads significantly without performing any down-regulation or sacrificing energy yield.

More details and methodology can be found in Deliverable Report D5.

Simulation results

The turbine model employed in this study is the DTU 10 MW [41]. The simulation is conducted based on nonlinear model derived using the parameters obtained from HAWCStab2. The model is of much greater complexity than the linear model employed for control design. Also,the DTU Wind Energy Controller [34, 43] is employed in this study. Closed-loop simulations were performed under a set of representative and turbulent wind fields generated based on the Mann model (Mann, 1998). These full-field three-dimensional wind data were characterized by mean wind speeds, turbulence settings and wind shear exponent. The mean wind speed is 15 m/s and the turbulence intensity is 10%.

Three control strategies were investigated:

1. Baseline: Feedback only based on DTU Wind Energy Controller;
2. MPC: Soft-constraint MPC without upcoming wind information. The only available wind measurement is the current hub-height wind speed;
3. MPC+FF: Feed-forward (FF) soft-constraint MPC. The feed-forward information is coming from 9 points LiDAR measurements, which is uniformly distributed across the rotor

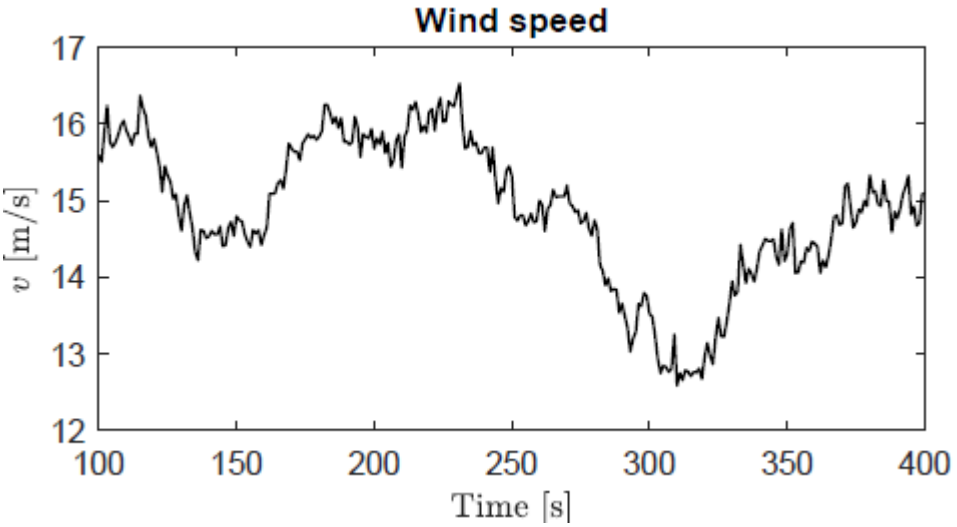

Figure 23 - Time series of the wind speed.

Figure 23 shows the time-series of the averaged wind speed experienced by the rotor. Figure 24

demonstrates the rotor speed and tower fore-aft displacement. Notice that a soft-constraint of 0.45 is imposed on the tower displacement. By inspecting the tower displacement, the MPC and MPC+FF both were able to predict constraint violations around 150 s and the tower position was able to maintain within 0.45 m. However, near 300 s, the MPC and MPC+FF could not keep the tower within the limit. This is reasonable for the MPC as the MPC does not have advance information. But that is surprising for the MPC+FF as this controller can foresee the wind speed. Further investigation should be conducted.

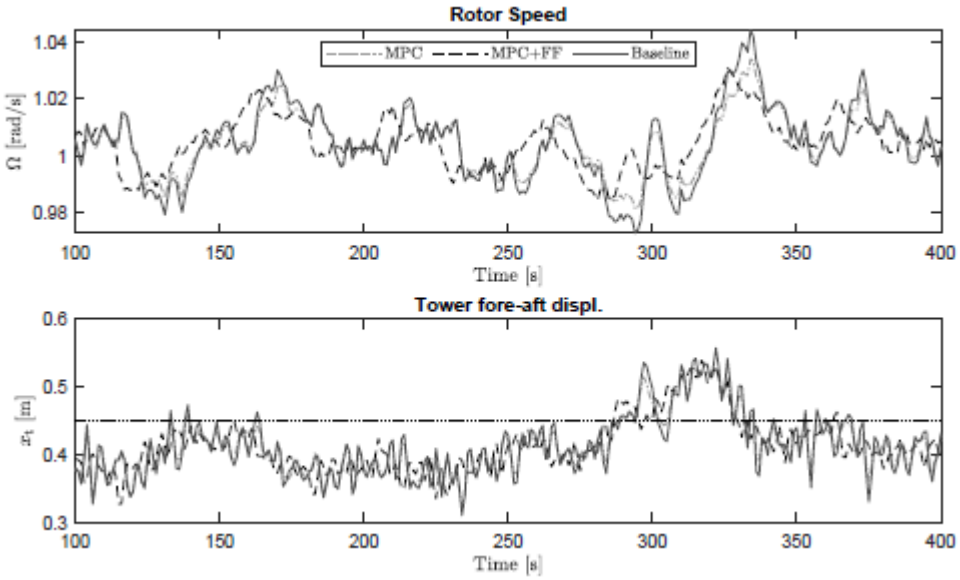

Figure 24 - Time series of the rotor speed and tower fore-aft displacement.

Figure 25 shows the pitch activities between the controllers. Figure 26 shows the input perturbation and slack variable. Notice that the input perturbation c mainly handles the constraint and feed-forward information. If the constraint is not active, the MPC performance should be the same as the baseline, that indicates the input perturbation should be zero. However, model mismatch might causes the MPC to predict some constraint violations that didn't happen. Thus, the control input of the MPC might be different to the baseline. Regarding the MPC+FF, it is obvious that the feed-forward information caused the MPC+FF control action behaved differently. Notice that the pitch rates of three controllers were quite low as the maximum pitch rate of typical pitch actuator is around 8-10 deg/s.

In Figure 26, it is interesting to see there was some activities in the slack variable, which is expected. Around 300 s, both MPC and MPC+FF could not handle the constraint on the tower

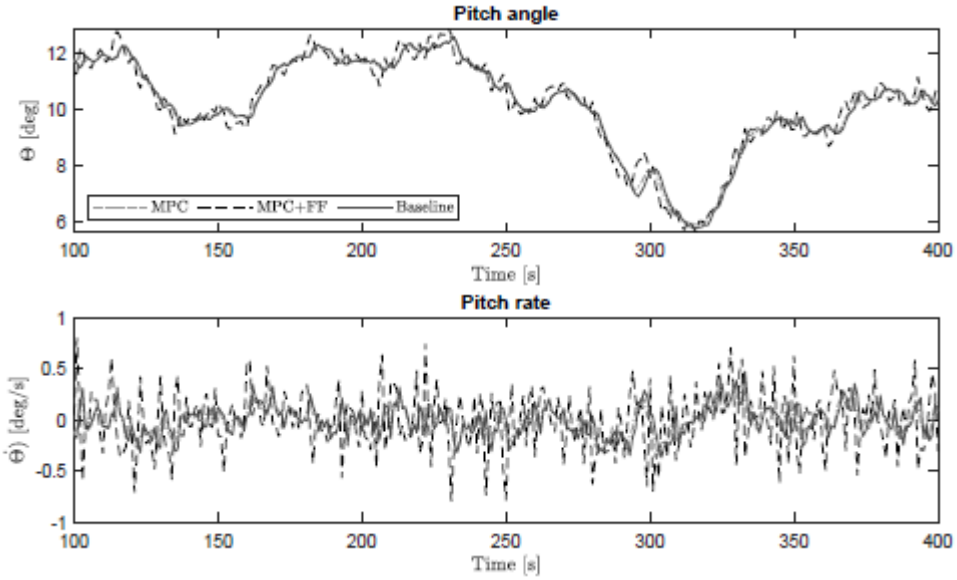

Figure 25 - Times series of the pitch angle and pitch rate.

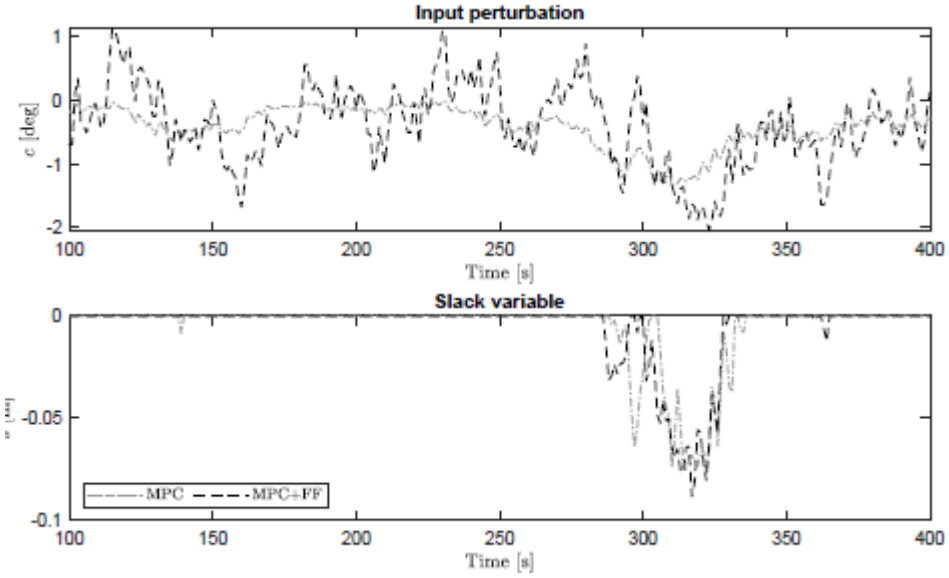

Figure 26 - Time series of the input perturbation and slack variable for soft-constraint handling.

5.7 Full-scale Turbine Measurement Champaign

This work investigates the wake under yaw set-point changes and turbine de-rating in a full-scale experimental turbine. Specifically, the tests are conducted on a Vestas V52 wind turbine located at Risø, Denmark. In wake steering campaign, the turbine is operated at static yaw offsets of

10,20,30 deg. In the de-rating campaign, the turbine is down-regulated at 80% and 60% of the rated power. The results from the measurement campaign were used in validating a wake tracking algorithm, where the wake centre position was estimated from four points of measurements of the wind scanner. In addition, the wake generated from a yawed turbine was also used in another wake studies. The data helped to validate different wake models.

More details can be found in Deliverable Report D6.

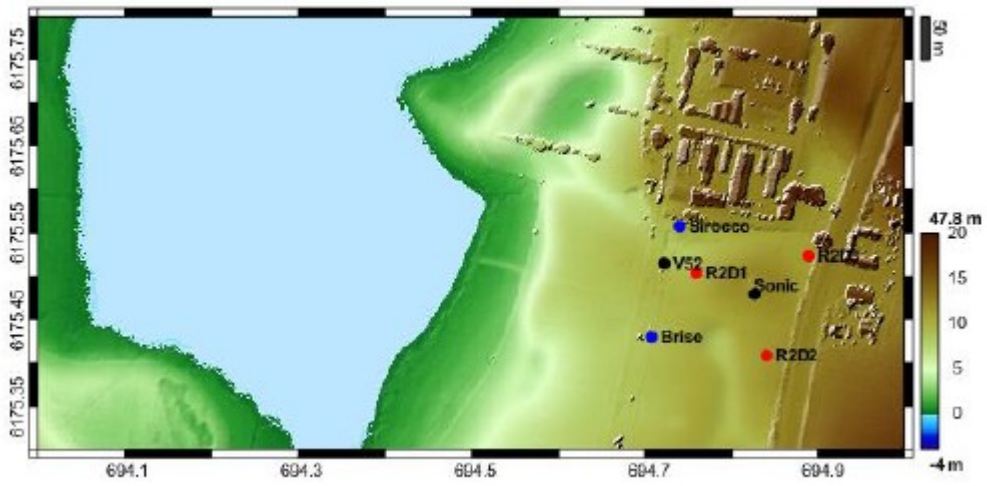

Figure 27 - Elevation map of the area where the experment was taking place. The coordinates are in UTM32 WGS84.

The PowerKey experiment was conducted with V52 wind turbine (WT), which is situated at northern most position of the row of turbines at the Risø test site. The test site comprises of two wind turbines and a rotating test rig. 120 m North-West of the V52 WT a 70 m meteorological mast is situated. The V52 WT is surrounded by grass land and fields. Buildings are located 60 m north of the V52 WT, and 190 m west of the V52 WT a main road runs north-south. West of the main road there is a forest of willow trees. The meteorological mast is positioned north-west of the V52 WT. The terrain follows a slopes of about 3 % down to the meteorological mast. Northwest of the meteorological mast the terrain has a steep slope down to Roskilde Fjord. Figure 27 shows an elevation map of the area, where the experiment took place.

Long range wind scanner (LRWS)

The LRWS is a coherent Doppler lidar based on a pulsed laser system. The LRWS consist of the commercial available Windcube 200 and a dual-axis mirror based steerable scan head[12] which enables the scanner to steer the beam in all directions. The beam is unfocused, and the probe length is determined by the length of the emitted pulse and the distance the pulse travels during the sampling of one Doppler spectrum. For this campaign a fft size of 64 and a pulse length 200 ns was used, which gives a probe length of about 38 m.
The two scanners was positioned 90 m apart, and a scan pattern scanning transects in three heights was synchronized in time and space. Range gates were chosen in distances from 50 m to 300mwith a distance of 50mbetween the range gates. Figure 2 and 3 shows the measurement points from each wind scanners seen down-streams from the turbine and from above.

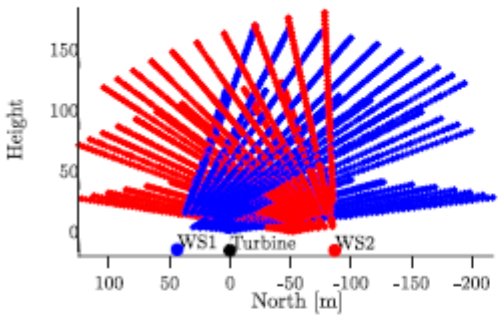

Figure 2. LRWS scan pattern seen from behind the turbine.

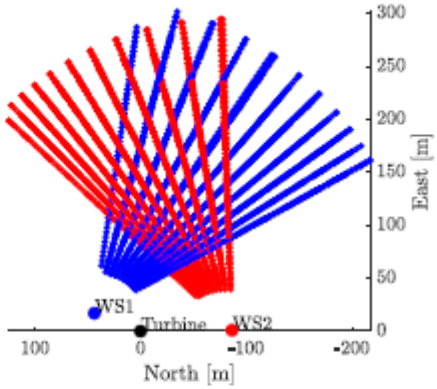

Figure 3. LRWS scan pattern seen from above.

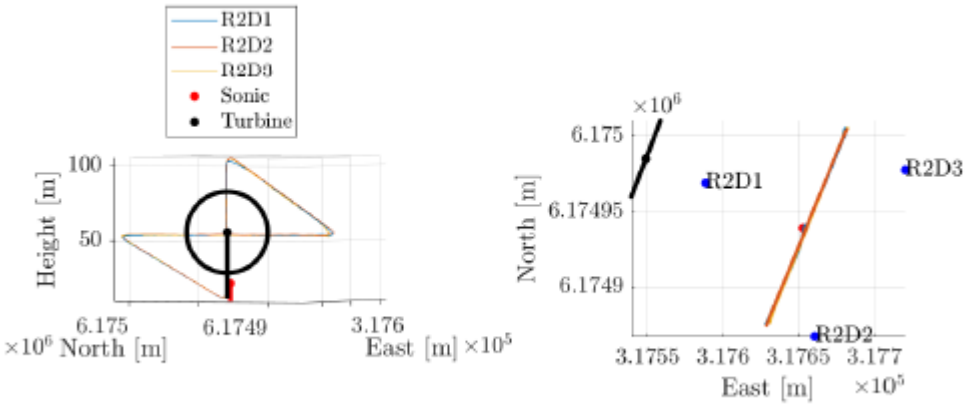

Figure 28 – Scan pattern for SRWS. Left pane: setup seen from the side. The turbine is in this case yawed in the direction 291 degrees. Right pane: SRWS setup seen from above.

Short Range Wind Scanner (SRWS)

The SRWS is based on a continuous wave (CW) lidar technology, where the measurement volume is defined by the focus position. A focus motor in the telescope enables the scanner to change the focus distance. The probe length increases quadratically with distance from the scanner, which limits the measuring distance to 150 m. The scan-head of the SRWS consist of two prisms which each deflect the laser beam 30_ giving a maximum deflection angle of 60_. Each prism is rotated using separate motors. Together with the focus motor this enables the scanner to move the measurement volume within a cone with an opening angle of 120_. The SRWS is only measuring in a single point, however it has a smaller measurement volume than the LRWS, making it possible to have faster sampling rate (up to 400 Hz). This makes it suitable for e.g. turbulence investigations. The measurement volume of the three SRWSs are controlled to be synchronised in time and space providing a 3D wind vector (u;v;w) in the position where the three beams intersect.
The scanners was setup to scan in a pattern similar to the scan pattern used in the the CCA campaign in 2018 (Tegtmeier, 2020). The scanners scan a cross perpendicular to the wind direction when the wind comes from 290_. Figure 28 shows the scan patterns for the three SRWSs. To optimize the scanning speed the four ends of the cross is connected by two diagonal lines. One pattern take about 1 seconds to be completed.

The scan speed is very depended on the alignment of the three scanners. In order to obtain the

fastest scanning speed the scanners had to be aligned such that the z-axis of the passing through the center of the cross. The alignment procedure is described in (Tegtmeier, 2020).

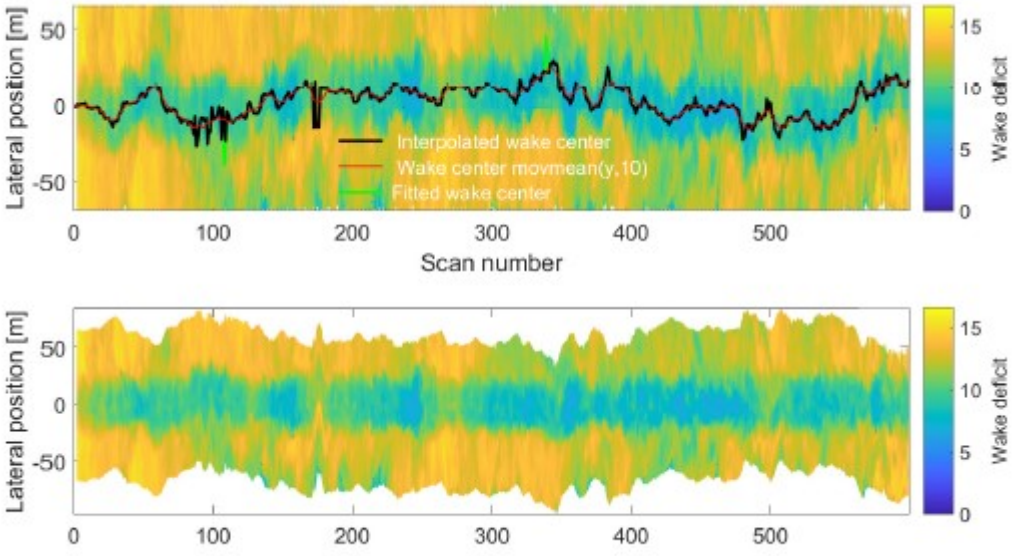

Figure 29 - Top figure: Horizontal cross section of the wake in the period 02-05-2019 in the time span 18:40-18:50. The green line indicates the fitted wake center, the black line is the fitted wake center with the outliers removed using an linear interpolation to fill replace the removed data and the red line shows an moving average over 10 scan numbers of the interpolated data. Bottom figure: Horizontal cross section of the wake in the period 02-05-2019 in the time span 18:40-18:50 where the lateral position have been subtracted the wake position from the red line in the above plot.

Yaw case

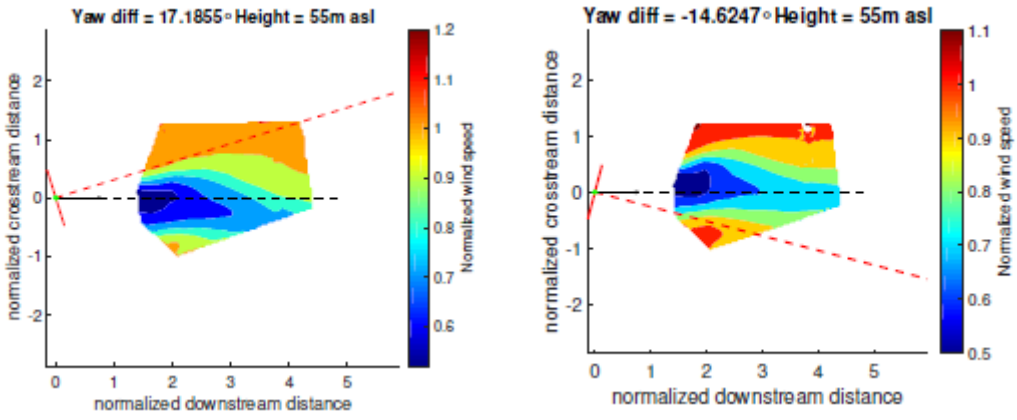

Figure 30 - Negative and zero yaw case. These are 10-min average.

Derating case

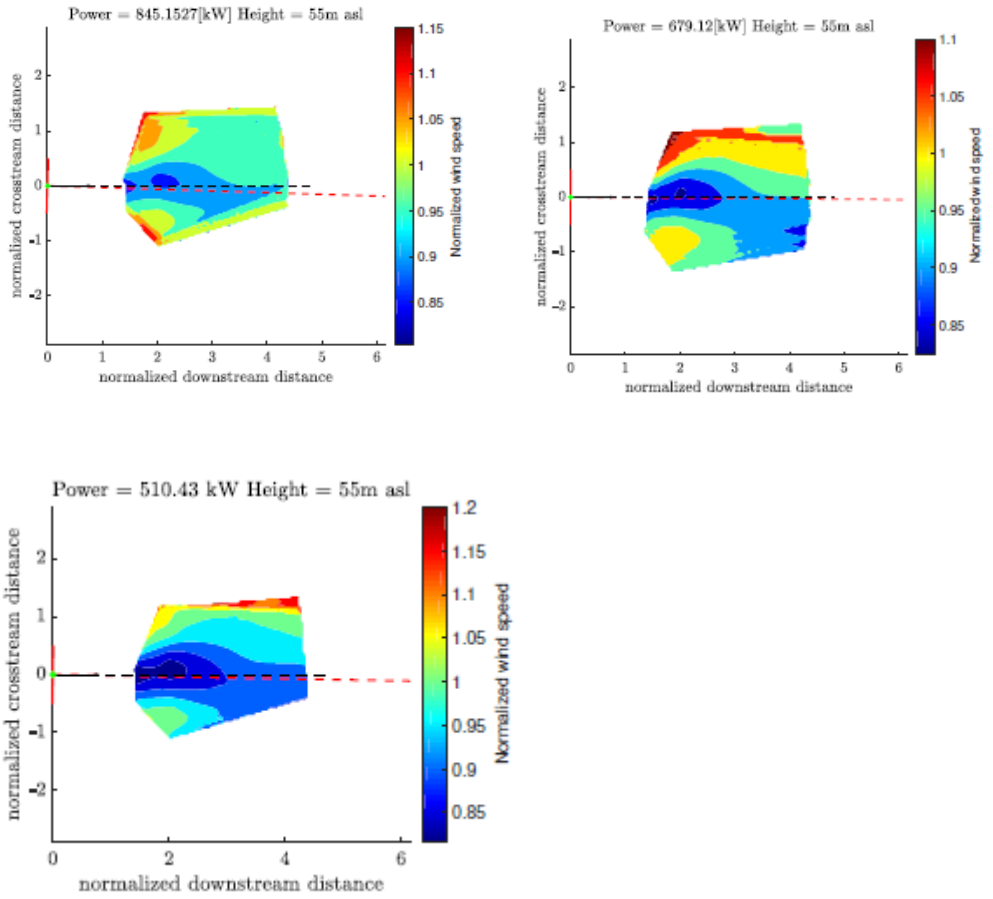

Figure 31- 100%, 80%, 60% derating case. These are 10-min average.

5.8 Publications from the project results

The project results have been presented in the following conferences:

1. Dong L & Lio WH (2021). Turbulence-based load alleviation control for wind turbine in extreme turbulence situation, European Control Conference 2021, Netherlands.
2. Lio WH, Larsen GC & Poulsen NK (2020) Dynamic wake tracking and characteristics estimation using a cost-effective lidar, TORQUE 2020, Netherlands.
3. Lio WH & Meng F (2020) Effective wind speed estimation for wind turbines in down-regulation, NAWEA WindTech 2019 14–16 October 2019, Amherst, MA USA.
4. Lio WH, Galinos C & Urban AM (2019) Analysis and design of gain-scheduling blade-pitch controllers for wind turbine down-regulation, 2019 IEEE 15th International Conference on Control and Automation (ICCA), Edinburgh, United Kingdom.
5. Galinos C, Urban AM & Lio WH (2019) Optimised de-rated wind turbine response and loading through extended controller gain-scheduling, WindEurope Conference and Exhibition 2019 2–4 April 2019, Bilbao, Spain.

6. Meng F & Lio WH (2020) The effect of minimum thrust coefficient control strategy on power output and loads of a wind farm, NAWEA WindTech 2019 Conference at University of Massachusetts, Amherst, USA.
7. Meng F, Lio WH & Barlas TK (2020) DTUWEC: an open-source DTU wind energy controller with advanced industrial features, Science of making torque from wind 2020, Delft, the Netherlands.
8. Lio WH, Mirzaei M Larsen GC (2018) On wind turbine down-regulation control strategies and rotor speed set-point, The Science of Making Torque from Wind (TORQUE2018),Milan, Italy, 20-23 Jun 2018.
9. Larsen, G. C., Ott, S., Liew, J., van der Laan, M. P., Simon, E., Thorsen, G. R., & Jacobs, P. (2020). Yaw induced wake deflection-a full-scale validation study. Science of making torque from wind 2020, Delft, the Netherlands.
10. Liang Lu, "Enhanced frequency control capability from wind turbine generators and wind power plants," in 2018 HVDC Colloquium, 2018.
11. Liang Lu, "Virtual synchronous machine control for wind turbines: a review," in 16th Deep Sea Offshore Wind R&D Conference, EERA DeepWind'2019, 2019.
12. Liang Lu, "A virtual synchronous machine control scheme for wind turbines," in Wind Energy Science Conference, WESC, 2019.
13. Liang Lu, "Power angle small-signal stability analysis of grid-forming wind turbine inverter based on VSM control," in 18th Wind Integration Workshop: International workshop on large-scale integration of wind power into power systems as well as on transmission networks for offshore wind power plants, 2019.
14. Liang Lu, "Power system frequency support of wind turbines with virtual synchronous machine control," in EAWE PhD Seminar, 2019.

In addition, some of the results have been published in reputable international journals and conference proceedings, and thus made available to the wider research community. The publications are listed as follows:

1. Lio WH, Larsen, GC & Thorsen GR (2021), Dynamic wake tracking using a cost-effective LiDAR and Kalman filtering: design, simulation and full-scale validation, Renewable Energy, accepted.
2. Dong L & Lio WH (2021). Turbulence-based load alleviation control for wind turbine in extreme turbulence situation, European Control Conference 2021.
3. Dong L, Lio WH & Meng F (2021), Wake position tracking using dynamic wake meandering model and rotor loads, Journal of Renewable and Sustainable Energy, in press.
4. Lio WH, Li A & Meng F (2021), Real-time rotor effective wind speed estimation using Gaussian process regression and Kalman filtering, Renewable Energy, in press.
5. Lio WH & Meng F (2020) Kalman-based interacting multiple-model wind speed estimator for wind turbines, IFAC 2020, In Press.
6. Lio WH, Larsen GC & Poulsen NK (2020) Dynamic wake tracking and characteristics estimation using a cost-effective lidar, in Journal of Physics: Conference Series, 1618,032036.
7. Lio WH & Meng F (2020) Effective wind speed estimation for wind turbines in down-regulation, in Journal of Physics: Conference Series, 1452,012008.
8. Lio WH, Galinos C & Urban AM (2019) Analysis and design of gain-scheduling blade-pitch controllers for wind turbine down-regulation, 2019 IEEE 15th International Conference on Control and Automation (ICCA), Edinburgh, United Kingdom, 2019, pp. 708-71.
9. Galinos C, Urban AM & Lio WH (2019) Optimised de-rated wind turbine response and loading through extended controller gain-scheduling, in Journal of Physics: Conference Series, 1222, 012020.

10. Meng F & Lio WH (2020) The effect of minimum thrust coefficient control strategy on power output and loads of a wind farm. In Journal of Physics: Conference Series.
11. Meng F, Lio WH & Barlas TK (2020) DTUWEC: an open-source DTU wind energy controller with advanced industrial features. In Journal of Physics: Conference Series.
12. Gasparis G, Lio WH & Meng F (2020) Surrogate Models for Wind Turbine Electrical Power and Fatigue Loads in Wind Farm, Energies.
13. Lio, W. H., Mirzaei, M., Larsen, G. C. (2018). On wind turbine down-regulation control strategies and rotor speed set-point. Journal of Physics: Conference Series, 1037, 032040.2.
14. Lio, W. H. (202x). Model predictive control on attenuating tower loads. In preparation
15. Larsen, G. C., Ott, S., Liew, J., van der Laan, M. P., Simon, E., Thorsen, G. R., & Jacobs, P. (2020). Yaw induced wake deflection-a full-scale validation study. Journal of Physics: Conference Series, 1618, 062047.
16. L. Lu, N. A. Cutululis, "Virtual synchronous machine control for wind turbines: a review," Proceedings of the 16th Deep Sea Offshore Wind R&D Conference, Journal of Physics: Conference Series (Online), vol. 1356, no. 012028, 2019.
17. L. Lu, Ö. Göksu, N. A. Cutululis, "Power angle small-signal stability analysis of grid-forming wind turbine inverter based on VSM control", Proceedings of the 18th wind integration workshop : International workshop on large-scale integration of wind power into power systems as well as on transmission networks for offshore wind power plants, 2019.

Some of the results have already been used in other research projects. For example, in the large-scale EU project (TotalControl). TotalControl uses some de-rating control methods developed in PowerKey. The methods and control solutions developed in this project are particularly relevant for wind turbine controller manufacturers. For example, Danish KK Wind Solution A/S and Mita Teknik A/S. In addition, it is useful for wind turbine manufacturers such as Vestas and Siemens.

One of the obstacles in the project was in WP2 experimental validation. As mentioned before, the test turbine controller could not be modified. Searching for an alternative turbine was beyond the timeline and budget of this project. The task was then focused on experiments that do not require major reconfiguration of the controller such as wake measurement with different power set-point and different yaw settings as well as verification of different estimation schemes.

6. Utilisation of project results

- *Describe how the obtained technological results will be utilised in the future and by whom.*
- *Describe how the obtained commercial results will be utilised in the future and by whom the results will be commercialised.*
  - *Did the project so far lead to increased turnover, exports, employment and additional private investments? Do the project partners expect that the project results in increased turnover, exports, employment and additional private investments?*
- *Describe the competitive situation in the market you expect to enter.*
  - *Are there competing solutions on the market? Specify who the main competitors are and describe their solutions.*
- *Describe entry or sales barriers and how these are expected to be overcome.*
- *How does the project results contribute to realise energy policy objectives?*

- *If Ph.D.'s have been part of the project, it must be described how the results from the project are used in teaching and other dissemination activities.*

The project results involve a wide range of control solutions for wind turbines that need to support the grid frequency and/or turbines that are located in a wind farm. By understanding the grid condition and the wind farm wind flow situation, turbines can produce higher power output and reduce the fatigue loads of key structural components. Thus, by achieving these objectives, the cost of wind energy will decrease.

There are a number of control methods developed and evaluated in this project. For example, down-regulation strategies, rotor effective wind speed estimator, turbulence-based control, frequency support control and model predictive control. These control solutions are implemented in the open-source DTU Wind Energy Controller. The controller toolbox can be downloaded and free access is offered anyone, for example, wind energy and control students, wind turbine and controller manufacturers or wind farm operators.

The project results have also been disseminated in academic journals (17 journal publication and conference proceedings) and presented in many (14) international conferences. Furthermore, some of the project results, for example, the down-regulation strategies, have been utilised in another research project, for example, the large-scale EU project (TotalControl).

Besides the control methods, this project also obtained some useful and valuable experimental wind measurement of the wake behind the Vestas V52 research turbine at Risø. The turbine was both down-regulated and misaligned with the dominant wind direction. The wind measurement data is important for understanding the wake behaviour of a yawed and down-regulated turbine, which in turn is useful for wind turbine and farm control.

In terms of user cases, the wind measurements were used by a DTU internal research project dealing with wake tracking. A wake tracking algorithm was developed by DTU, and the PowerKey measurement data were used for experimental validation purposes.

The market for control solutions is relatively secretive, since most of the wind turbine manufacturers developed their in-house control strategies. Despite that, the project results are valuable for wind turbine controller developers such as Mita Teknik A/S and KK Wind Solutions A/S. In the future, based on the control methods developed by PowerKey, DTU can propose other research projects with Danish wind turbine controller developers or/and wind turbine manufacturers.

The developed and tested control solutions developed by PowerKey can contribute to realising the energy policy objective. The proposed control solutions can boost wind power output per wind turbine and also extend the lifetime of key structural components of the turbines. Furthermore, the turbines can adapt to the grid condition and provide ancillary services. All these factors can be translated to lower cost of wind energy. Thus, it is beneficial for the wind turbine manufacturers, the wind farm operator and the electricity users, namely, the households.

7. Project conclusion and perspective

- *State the conclusions made in the project.*
- *What are the next steps for the developed technology?*
- *Put into perspective how the project results may influence future development*

In conclusion, the outcome of PowerKey is fruitful. The project developed and tested many control methods for turbines adapting these to the grid and wind farm conditions. For example, down-regulation strategies, rotor

effective wind speed estimator, turbulence-based control and model predictive control and more. Moreover, the experimental test was also conducted using the Vestas V52 research turbine at Risø. Wind measurements have been obtained from the turbine operated in a down-regulated and yawed state, which are particularly valuable for understanding wind turbine and farm control in the future.

Furthermore, the project results have been disseminated in a wide range of reputable journals and presented in many international conferences (17 publications and 14 conferences). The developed control methods are also freely available in the open-source DTU Wind Energy Controller, which is beneficial for the next generation of wind energy and control students world-wide, wind turbine manufacturers and wind turbine controller developers.

The next steps for the developed control technology in this project are limitless. A possible step is that DTU will develop research proposals with other Danish/EU partners based on the developed control methods, thus, ensuring the developed control strategies getting into a bigger and wider market. Some of the project results (e.g. down-regulation strategies and field measurement data) have already been using in other research projects (e.g. in the large-scale EU project TotalControl) as well as in a DTU internal project.

8. Appendices

8.1 References

Aho, J., Buckspan, A., & Laks, J. H. (2012). A tutorial of wind turbine control for supporting grid frequency through active power control. *Proc. of the American Control Conference*, 3120–3131. https://doi.org/10.1109/ACC.2012.6315180

Bak, C., Zahle, F., Bitsche, R., & Kim, T. (2013). The DTU 10-MW reference wind turbine. *Danish Wind Power Research 2013*. http://orbit.dtu.dk/services/downloadRegister/55645274/

Hansen, M. H., & Henriksen, L. C. (2013). Basic DTU Wind Energy controller. In *DTU Wind Energy* (Issue January).

IEC. (2005). *IEC 61400-1 Ed.3: Wind turbines - Part 1: Design requirements*. *2005*.

Lio, A. W. H., & Meng, F. (2020). Effective wind speed estimation for wind turbines in down-regulation. *Journal of Physics: Conference Series*, *1452*, 012008. https://doi.org/10.1088/1742-6596/1452/1/012008

Lio, W. H., Galinos, C., & Urban, A. M. (2019). Analysis and design of gain-scheduling blade-pitch controllers for wind turbine down-regulation *. *2019 IEEE 15th International Conference on Control and Automation (ICCA)*, 708–712. https://doi.org/10.1109/ICCA.2019.8899611

Lio, W. H., Mirzaei, M., & Larsen, G. Chr. (2018). On wind turbine down-regulation control strategies and rotor speed set-point. *Journal of Physics: Conference Series*, *1037*, 032040. https://doi.org/10.1088/1742-6596/1037/3/032040

Lu, L., Saborío-Romano, O., & Cutululis, N. A. (2021). Reduced-Order-VSM-Based Frequency Controller for Wind Turbines. *Energies*, *14*(3), 528. https://doi.org/10.3390/en14030528

Ma, K., Zhu, J., Soltani, M., Hajizadeh, A., & Chen, Z. (2017). Wind turbine down-regulation strategy for minimum wake deficit. *2017 11th Asian Control Conference (ASCC)*, 2652–2656. https://doi.org/10.1109/ASCC.2017.8287595

Mann, J. (1998). Wind field simulation. *Probabilistic Engineering Mechanics*, *13*(4), 269–282. https://doi.org/10.1016/S0266-8920(97)00036-2

Meng, F., Lio, A. W. H., & Liew, J. (2020). The effect of minimum thrust coefficient control strategy on power output and loads of a wind farm. *Journal of Physics: Conference Series*, *1452*(1). https://doi.org/10.1088/1742-6596/1452/1/012009

Mirzaei, M., Soltani, M., Poulsen, N. K., & Niemann, H. H. (2014). Model based active power control of a wind turbine. *2014 American Control Conference*, *July 2016*, 5037–5042. https://doi.org/10.1109/ACC.2014.6859055

Tegtmeier, A. (2020). 2018 V52-CCA Shortrange Windscanner. *DTU Wind Energy E-Report-0198*.

Tibaldi, C., Hansen, M. H., & Zahle, F. (2015). Methods for systematic tuning of wind turbine controllers. *DTU Wind Energy Report E-0100 (EN)*, 1–21.

Zhu, J., Ma, K., Soltani, M., Hajizadeh, A., & Chen, Z. (2017). Comparison of loads for wind turbine down-regulation strategies. *2017 11th Asian Control Conference (ASCC)*, 2784–2789. https://doi.org/10.1109/ASCC.2017.8287618